This is an Accepted Manuscript of an article published by Taylor & Francis in the Journal of Building Performance Simulation on 06 April 2022, available at: http://www.tandfonline.com/10.1080/19401493.2022.2058087.

Chance Constrained Stochastic MPC for Building Climate Control under Combined Parametric and Additive Uncertainty

Anke Uytterhoeven[1,2], Robbe Van Rompaey[3], Kenneth Bruninx[1,2], and Lieve Helsen[1,2]

[1]KU Leuven, Department of Mechanical Engineering, Division of Applied Mechanics and Energy Conversion, Celestijnenlaan 300 box 2421, 3001 Leuven, Belgium.
[2]EnergyVille, Thor Park 8310, 3600 Genk, Belgium.
[3]KU Leuven, Department of Electrical Engineering, STADIUS, Kasteelpark Arenberg 10 box 2446, 3001 Leuven, Belgium.

Abstract

This paper presents a chance constrained stochastic model predictive control (SMPC) approach for building climate control under combined parametric and additive uncertainties. The proposed SMPC^{ap} approach enables the quantification, and manipulation, of both the mean and covariance of the stochastic system states and inputs. Its enhanced uncertainty anticipation is shown to induce improved thermal comfort in closed-loop simulations compared to the conventional deterministic MPC (DMPC) and the state-of-the-art SMPC^{a} only accounting for additive uncertainties, at the cost of a maximum relative increase in energy use of 21.6% and 4.2%, respectively. By incorporating the SMPC^{ap} strategy in an integrated optimal control and design (IOCD) approach, its additional added value for obtaining a more appropriate, yet robust, heat supply system sizing is illustrated. Via simulations, size reductions up to 33.3% are shown to be achievable for a terraced single-family dwelling without increasing thermal discomfort compared to an IOCD approach incorporating DMPC.

Keywords

Stochastic model predictive control, chance constraints, parametric uncertainty, additive uncertainty, building climate control, thermostatically controlled loads

List of abbreviations

ADF Affine disturbance feedback

DMPC Deterministic model predictive control

HVAC Heating, ventilation, and air conditioning

IOCD Integrated optimal control and design

MPC Model predictive control

OCP Optimal control problem

PBMPC Performance bound model predictive control

RMI Royal Belgian Meteorological Institute

RMPC Robust model predictive control

SMPC Stochastic model predictive control

SMPC^{ap} Stochastic model predictive control accounting for both additive and parametric uncertainties

SMPC^{a} Stochastic model predictive control accounting for additive uncertainties

SSM State space model

TCV Thermal comfort violations

TED Thermal energy demand

WDM Weighted distance to the mean

1 Introduction

Advanced control strategies for residential space heating, and model predictive control (MPC) in particular, are gaining widespread attention, since they can systematically save energy and/or costs with simultaneous thermal comfort improvement [1–5], as well as adapt the energy demand in correspondence with the available (renewable) electricity supply [6–9]. The performance of any MPC strategy is dependent on the accuracy of the mathematical model describing the thermal loads, and of the forecasts of disturbances, such as weather and occupant behavior. Deviating model parameters and inaccurate disturbance predictions may give rise to increased energy costs and comfort violations if not properly accounted for [10–13].

Within MPC literature, two main methods have been studied to explicitly address uncertainty: robust MPC (RMPC) and stochastic MPC (SMPC)[1] [14–18]. RMPC is tailored to systems subject to bounded uncertainty. It computes a control policy that guarantees constraint satisfaction for all possible uncertainty realizations, that are treated as equally likely, by optimizing the objective for the worst possible uncertainty realization. Hence, the resulting control strategy is rather conservative. SMPC, on the other hand, is tailored to systems subject to probabilistic uncertainty. It exploits the shape of the probability distributions to find a suitable control strategy under uncertainty, and allows for acceptable levels of constraint violations during system operation, as set by the user according to his risk averseness, by imposing probabilistic (chance) constraints, instead of hard constraints.

Both RMPC and SMPC applications for building climate control currently mainly focus on the uncertainty on the weather forecasts (typically ambient temperature and solar heat gains) and/or occupant behavior forecasts (typically equipment-related and metabolic internal heat gains) [17–24]. Although the building model parameters are recognized as another important source of uncertainty influencing the building energy performance [25, 26], this uncertainty is only occasionally explicitly addressed [27–30]. Nevertheless, the building controller model is not always capable of capturing the building dynamics in detail, due to the unavailability of sufficient data and/or experts' knowledge to set up the model[2], and/or due the impossibility to correctly describe the complexity of the underlying physics[3] [25, 30–32]. In that case, the parametric uncertainty of the controller model can become non-negligible, and hence, should be accounted for by the MPC strategy.

The careful consideration of all relevant uncertainties in the MPC strategy is not only relevant in an optimal control context, but also in an optimal design context, because of the close interconnection between both [33]. Indeed, the building envelope design determines the heating and cooling load profiles, and thus, which control actions are required, whereas the heating, ventilation, and air conditioning (HVAC) system design determines the technical limits of the heat supply, distribution and emission system, and thus, which control actions are possible. In recent years, there has been an emerging interest to also exploit optimal control algorithms for optimal design applications. A better alignment of control and design via an integrated optimal control and design (IOCD) methodology, properly accounting for the system dynamics, can result in a more appropriate, i.e., less oversized and more cost-optimal, system design [33, 34]. This is in sharp contrast with current engineering practices, which typically consider worst-case static conditions, as formulated in heat loss calculations (e.g., following NBN EN ISO 15251 [35]) and/or assign a safety factor to a deterministic load calculated for specific design conditions (see e.g., [36–40]). In the latter approach, this safety factor serves to account for more extreme situations than the design conditions, thereby implicitly dealing with uncertainty. An important issue associated with these kind of static approaches is that they may lead to oversized systems [36–40]. Although the transition towards IOCD methodologies is a considerable improvement tackling the oversize problem of the static approaches, there is risk that they still result in an inadequate system sizing, since current IOCD approaches typically overlook the impact of uncertainties. This could endanger the required thermal

[1] MPC strategies that take into account uncertainty in a more implicit way, such as offset-free MPC, adaptive MPC and learning-based MPC, are not considered here. For a detailed review on these methods, see [3].

[2] This is especially relevant in case of a large-scale roll-out of smart meters and controllers, also involving the older, existing building stock.

[3] In a residential context, it is not realistic to run large, non-linear optimization models on a thermostat; although the computations could be done on a server, this may not be cost-efficient.

comfort, and might moreover drastically reduce the flexibility potential needed in demand response programs. These problems could be overcome by using an RMPC or SMPC strategy for the optimal control part of the IOCD approach.

Given these trends and challenges, the main aim, and main novelty, of this work are to develop and assess an SMPC^{ap} strategy for building climate control under combined parametric (model)[4] and additive (disturbance forecast) uncertainty, which can be used for both optimal control and optimal design applications. The choice to pursue a stochastic rather than a robust approach is motivated by the fact that thermal comfort is allowed to be occasionally violated, which is confirmed in building standards (see e.g., [35, 41]), and by the probabilistic descriptions found in literature for the building envelope characteristics [31,36,42–44], weather conditions [23,26,36,45] and occupant behavior [26, 36, 44]. The presented approach is tailored to the class of systems represented by a linear time-invariant state space model (SSM).

The following research questions will be answered.
RQ 1: How does the nominal, deterministic optimal control problem (OCP) formulation for building climate control need to be reformulated in order to explicitly account for additive (disturbance forecast) and parametric (model) uncertainties?
RQ 2: How can all relevant uncertainties affecting the building climate be appropriately mathematically modelled in order to include them in the stochastic OCP formulation?
RQ 3: Does the SMPC^{ap} strategy guarantee a better control performance than the current-practice deterministic MPC strategy, and the state-of-the-art SMPC^{a} strategy only accounting for additive uncertainties?
RQ 4: Does the SMPC^{ap} strategy allow reducing the HVAC system size with the same probabilistic guarantees of thermal comfort when embedded in an integrated optimal control and design approach?

The first two research questions, covering the two main aspects of the SMPC^{ap} development, are answered in Section 2. First, the nominal, deterministic OCP, presented in Section 2.2, is reformulated into its stochastic equivalent in Section 2.3.1. Here, analytically reformulated chance constraints are combined with affine disturbance feedback (ADF) to reduce conservatism. Next, the mathematical uncertainty characterization, serving as an essential part of the stochastic OCP formulation, is derived in Section 2.3.2. To fully appraise the possible added value of the SMPC^{ap} strategy, its performance is assessed in two case studies, presented in Section 2.4, aiming to answer the remaining research questions with the help of simulations. The main focus of the first case study is on the attainable thermal comfort improvement by hedging against uncertainty in an optimal control context. The second case study illustrates the usability of the SMPC^{ap} strategy for obtaining a more appropriate, yet robust, sizing of the heating system in an optimal design context. The results of these two case studies are discussed in detail in Section 3, after which conclusions are drawn in Section 4.

2 Methods

In this section, first, a short overview of the relevant notation is given in Section 2.1. Then, the deterministic MPC formulation is introduced in Section 2.2. Subsequently, the stochastic substitute is systematically derived in Section 2.3, by reformulating the OCP in Section 2.3.1 and by introducing the mathematical uncertainty characterization in Section 2.3.2. Finally, in Section 2.4, the case studies to assess the potential added value of the proposed SMPC^{ap} approach are presented.

2.1 Notation

Bolt face upper case letters refer to matrices, bolt face lower case letters refer to vectors, and regular lower case letters refer to scalars. Letters with superscript tilde $\tilde{.}$ refer to uncertain parameters or variables with mean $\bar{.}$ and uncertain portion $\delta.$, representing the unknown deviation of the stochastic parameter/variable from its mean value. $\mathbb{E}[.]$ is the expected value operator, $P(.)$ represents a probability. $\mathbb{R}$ represents the set of real numbers, and $\mathbb{N}$ the set of integer numbers. $\mathbf{0}_{i\times j}$ is the $i \times j$ zero matrix, $\mathbf{0}_i$ is an all-zeros vector of size i, $\mathbf{I}_i$ is the $i \times i$ identity matrix, $\mathbf{1}_i$ is an all-ones vector of size i, and $\mathbf{e}_i$ is a selection vector containing a one on the ith position and zeros elsewhere. $vec(.)$ denotes the vectorization of a matrix stacking all its columns in one vector. $\otimes$ denotes

[4] The uncertainty about the building model is limited to parametric uncertainty, i.e., uncertainty about the value of the model parameters. Model-form uncertainty, representing the discrepancy between the complex physical process and the simplified mathematical characterization, is out of scope of this work.

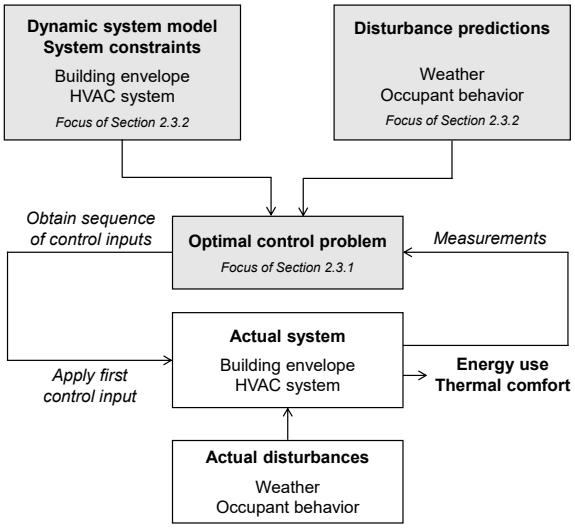


Figure 1: The general MPC procedure for building climate control. All relevant parts regarding the SMPC development, which is the focus of this work, are highlighted in grey. Adapted from [46].

the Kronecker product.

2.2 Problem formulation

Figure 1 illustrates the general MPC procedure for building climate control. At the current point in time, the heating plan for the next several hours up to days is determined by solving an open-loop optimal control problem. This open-loop OCP aims at optimizing the heating system operation over a finite prediction horizon in accordance with a selected objective function (e.g., minimization of energy use, operational cost, CO_2 emission, ... and/or maximization of thermal comfort), while explicitly taking into account the mathematical model representing the system behavior together with predictions of the relevant boundary conditions.

The nominal, deterministic open-loop OCP for the class of systems represented by a linear time-invariant SSM can be mathematically formulated as follows.

$$\min_{\substack{\{\mathbf{x}_k\}_{k=0\dots K+1},\\ \{\mathbf{s}_k\}_{k=0\dots K+1},\\ \{\mathbf{u}_k\}_{k=0\dots K}}} \quad \phi\left(\mathbf{x}_k, \mathbf{s}_k, \mathbf{u}_k\right)$$

$$s.t.\ \mathbf{x}_{k+1} = \mathbf{A}\,\mathbf{x}_k + \mathbf{B}\,\mathbf{u}_k + \mathbf{E}\,\mathbf{d}_k \quad \forall k \qquad (1a)$$

$$\mathbf{x}_k + \mathbf{s}_k \geq \mathbf{x}_k^{min} \quad \forall k \qquad (1b)$$

$$\mathbf{x}_k - \mathbf{s}_k \leq \mathbf{x}_k^{max} \quad \forall k \qquad (1c)$$

$$\mathbf{s}_k \geq \mathbf{0}_{n_x} \quad \forall k \qquad (1d)$$

$$\mathbf{0}_{n_u} \leq \mathbf{u}_k \leq \mathbf{u}_k^{max} \quad \forall k \qquad (1e)$$

$$\mathbf{x}(0) = \mathbf{x}_0 \qquad (1f)$$

$$\mathbf{u}(0) = \mathbf{u}_0 \qquad (1g)$$

Here, $\{\mathbf{x}_k \in \mathbb{R}^{n_x}\}_{k=0\dots K+1}$ represents all system states over the prediction horizon K, being the indoor temperature as well as all relevant temperatures of the building construction elements and of the HVAC system. $\{\mathbf{s}_k \in \mathbb{R}^{n_x}\}_{k=0\dots K+1}$ represents the slack variables relaxing the state constraints. $\{\mathbf{u}_k \in \mathbb{R}^{n_u}\}_{k=0\dots K}$ in turn represents the thermal power inputs delivered by the heat supply system during one time step Δt. Finally, $\{\mathbf{d}_k \in \mathbb{R}^{n_d}\}_{k=0\dots K}$ represents the predicted disturbances affecting the system, such as weather and occupant behavior.

The state space equation (1a) describes the dynamics of the building envelope and HVAC system with the help of the state space matrices $\mathbf{A} \in \mathbb{R}^{n_x \times n_x}$, $\mathbf{B} \in \mathbb{R}^{n_x \times n_u}$ and $\mathbf{E} \in \mathbb{R}^{n_x \times n_d}$, constituting the building controller model. This constraint determines the evolution of the system states $\mathbf{x}_{k+1}$ as a function of the preceding states $\mathbf{x}_k$, heat inputs $\mathbf{u}_k$ and disturbances $\mathbf{d}_k$. The states are constrained by a minimum and maximum bound, $\{\mathbf{x}_k^{min}\}_{k=0\dots K+1}$ and $\{\mathbf{x}_k^{max}\}_{k=0\dots K+1}$, in Equations (1b) and (1c). When applied to the indoor temperature, these state constraints denote the thermal comfort requirements. To ensure feasibility, even under the most adverse conditions, we introduce the slack variables $\mathbf{s}_k$ that are penalized in the pursued objective function ϕ at a very high cost. The inputs are in turn limited by a maximum power bound $\{\mathbf{u}_k^{max}\}_{k=0\dots K}$ in Equation (1e), which is typically reflecting the technical limits of the HVAC system. Finally, the current conditions, represented by $\mathbf{x}_0$ and $\mathbf{u}_0$, are taken into account as initial values for the states and inputs in Equations (1f) and (1g).

Typically, MPC algorithms are implemented in closed-loop, using the principle of receding horizon control, as shown in Figure 1. After solving the open-loop OCP, the first step of the optimized control sequence is applied to the building. Then, the actual system response is measured and fed back to the OCP, thereby

serving as an updated initial condition for the optimization at the next time step [3]. Although closed-loop MPC already offers a certain degree of robustness to uncertainties via the feedback mechanism, its nominal, deterministic OCP formulation (1), which is considering the system model $\mathbf{A}, \mathbf{B}, \mathbf{E}$ and disturbance predictions $\mathbf{d}_k$ as perfect representations of reality, typically fails to systematically deal with the impact of uncertainties [47]. Therefore, it is required to additionally adapt the formulation of the open-loop OCP by integrating information about the uncertainties in the problem formulation. This is the focus of the next subsection.

2.3 SMPC development

Uncertainties turn the parameters of the building controller model and the disturbance predictions into stochastic quantities, whose distribution can be characterized by a mean value and a covariance.

$$\mathbf{A} \rightarrow \tilde{\mathbf{A}} \triangleq \bar{\mathbf{A}} + \delta\mathbf{A}$$
$$\text{with } \bar{\mathbf{A}} \triangleq \mathbb{E}[\tilde{\mathbf{A}}]$$
$$\Sigma_{\mathbf{A}} \triangleq \mathbb{E}[\text{vec}(\delta\mathbf{A})\,\text{vec}(\delta\mathbf{A})^T] \tag{2a}$$
$$\mathbf{B} \rightarrow \tilde{\mathbf{B}} \triangleq \bar{\mathbf{B}} + \delta\mathbf{B} \tag{2b}$$
$$\mathbf{E} \rightarrow \tilde{\mathbf{E}} \triangleq \bar{\mathbf{E}} + \delta\mathbf{E} \tag{2c}$$
$$\mathbf{d}_k \rightarrow \tilde{\mathbf{d}}_k \triangleq \bar{\mathbf{d}}_k + \delta\mathbf{d}_k \quad \forall k \tag{2d}$$

In the first part of this subsection, it is shown how these probabilistic parametric $(\tilde{\mathbf{A}}, \tilde{\mathbf{B}}, \tilde{\mathbf{E}})$ and additive $(\tilde{\mathbf{d}}_k)$ uncertainties can be introduced in the OCP formulation for building climate control. Starting from the nominal, deterministic formulation, the stochastic substitute is derived in a convex form, provided that the original formulation is convex. This derivation is performed in a systematic way, by successively introducing the uncertainties in all relevant parts of the OCP.

2.3.1 Stochastic OCP formulation

Introducing uncertainties in the state space equation

By incorporating the uncertainties in the deterministic OCP (1), the deterministic state space equation (1a) is transformed into its stochastic counterpart

$$\begin{aligned}\tilde{\mathbf{x}}_{k+1} =& \tilde{\mathbf{A}}\,\tilde{\mathbf{x}}_k + \tilde{\mathbf{B}}\,\mathbf{u}_k + \tilde{\mathbf{E}}\,\tilde{\mathbf{d}}_k \\ =& (\bar{\mathbf{A}} + \delta\mathbf{A})(\bar{\mathbf{x}}_k + \delta\mathbf{x}_k) + (\bar{\mathbf{B}} + \delta\mathbf{B})\mathbf{u}_k + \\ & (\bar{\mathbf{E}} + \delta\mathbf{E})(\bar{\mathbf{d}}_k + \delta\mathbf{d}_k) \\ \approx& (\bar{\mathbf{A}}\,\bar{\mathbf{x}}_k + \bar{\mathbf{B}}\,\mathbf{u}_k + \bar{\mathbf{E}}\,\bar{\mathbf{d}}_k) + \\ & (\delta\mathbf{A}\,\bar{\mathbf{x}}_k + \bar{\mathbf{A}}\,\delta\mathbf{x}_k + \delta\mathbf{B}\,\mathbf{u}_k + \delta\mathbf{E}\,\bar{\mathbf{d}}_k + \bar{\mathbf{E}}\,\delta\mathbf{d}_k)\end{aligned} \tag{3}$$

where the second-order perturbations are neglected in the third step.

Because of the explicit dependency of the states $\mathbf{x}_k$ on the introduced uncertainties, imposed by the state space equation, the states are also transformed to stochastic variables. Based on Equation (3), the mean and covariance can then be allocated as

$$\bar{\mathbf{x}}_{k+1} = \bar{\mathbf{A}}\,\bar{\mathbf{x}}_k + \bar{\mathbf{B}}\,\mathbf{u}_k + \bar{\mathbf{E}}\,\bar{\mathbf{d}}_k \tag{4}$$

and

$$\begin{aligned}&\Sigma_{\mathbf{x}_{k+1}} \\ &= \mathbb{E}[(\delta\mathbf{A}\,\bar{\mathbf{x}}_k + \bar{\mathbf{A}}\,\delta\mathbf{x}_k + \delta\mathbf{B}\,\mathbf{u}_k + \delta\mathbf{E}\,\bar{\mathbf{d}}_k + \bar{\mathbf{E}}\,\delta\mathbf{d}_k) \\ &\qquad (\delta\mathbf{A}\,\bar{\mathbf{x}}_k + \bar{\mathbf{A}}\,\delta\mathbf{x}_k + \delta\mathbf{B}\,\mathbf{u}_k + \delta\mathbf{E}\,\bar{\mathbf{d}}_k + \bar{\mathbf{E}}\,\delta\mathbf{d}_k)^T],\end{aligned} \tag{5}$$

serving as the stochastic substitute for Equation (1a).

Note that the inputs $\mathbf{u}_k$, in contrast to the states, do not explicitly depend on any of the imposed uncertainties. Hence, for now, the deterministic form of the inputs is retained, but this will be revisited when introducing the uncertainties in the input constraints.

Further elaboration of Equation (5) in its current form would result in a non-convex expression, due to the cross-products of optimization variables. To overcome this issue, two manipulations are proposed in this work to convexify the constraint: the introduction of a latent variable aggregating all uncertainties, and a transformation of the covariance by using a square root notation.

First, all stochastic quantities are aggregated in the latent random variable $\tilde{\mathbf{p}} \in \mathbb{R}^{n_p}$ with mean $\bar{\mathbf{p}}$ and covariance $\Sigma_{\mathbf{p}}$, i.e.,

$$vec(\tilde{\mathbf{A}}) = \mathbf{T}_{\mathbf{A}}\,\tilde{\mathbf{p}} \text{ with } \mathbf{T}_{\mathbf{A}} \in \mathbb{R}^{n_x^2 \times n_p} \tag{6a}$$
$$vec(\tilde{\mathbf{B}}) = \mathbf{T}_{\mathbf{B}}\,\tilde{\mathbf{p}} \text{ with } \mathbf{T}_{\mathbf{B}} \in \mathbb{R}^{n_x n_u \times n_p} \tag{6b}$$
$$vec(\tilde{\mathbf{E}}) = \mathbf{T}_{\mathbf{E}}\,\tilde{\mathbf{p}} \text{ with } \mathbf{T}_{\mathbf{E}} \in \mathbb{R}^{n_x n_d \times n_p} \tag{6c}$$
$$\tilde{\mathbf{d}}_k = \mathbf{T}_{\mathbf{d}_k}\,\tilde{\mathbf{p}} \text{ with } \mathbf{T}_{\mathbf{d}_k} \in \mathbb{R}^{n_d \times n_p} \quad \forall k \tag{6d}$$

where $\mathbf{T}_{\mathbf{A}}, \mathbf{T}_{\mathbf{B}}, \mathbf{T}_{\mathbf{E}}$ and $\mathbf{T}_{\mathbf{d}_k}$ are appropriate selection matrices. Consequently, any stochastic parameter $\tilde{\mathbf{f}} \in \{\tilde{\mathbf{A}}, \tilde{\mathbf{B}}, \tilde{\mathbf{E}}, \tilde{\mathbf{d}}_k\}$ can be expressed as

$$vec(\tilde{\mathbf{f}}) = vec(\bar{\mathbf{f}}) + vec(\delta\mathbf{f}), \tag{7}$$

with

$$vec(\bar{\mathbf{f}}) = \mathbb{E}[vec(\tilde{\mathbf{f}})] = \mathbf{T_f}\,\bar{\mathbf{p}} \tag{8a}$$

and

$$\Sigma_{\mathbf{f}} = \mathbb{E}[vec(\delta\mathbf{f})\,vec(\delta\mathbf{f})^T] = \mathbf{T_f}\,\Sigma_{\mathbf{p}}\,\mathbf{T_f}^T \tag{8b}$$

being the (vectorized) mean and covariance of $\tilde{\mathbf{f}}$. Besides, the covariance between two stochastic quantities $\tilde{\mathbf{f}}, \tilde{\mathbf{g}} \in \{\tilde{\mathbf{A}}, \tilde{\mathbf{B}}, \tilde{\mathbf{E}}, \tilde{\mathbf{d}}_k\}$ that are correlated with one another, can be written as

$$\Sigma_{\mathbf{f},\mathbf{g}} = \mathbb{E}[vec(\delta\mathbf{f})\,vec(\delta\mathbf{g})^T] = \mathbf{T_f}\,\Sigma_{\mathbf{p}}\mathbf{T_g}^T. \tag{9}$$

Second, the covariance matrix $\Sigma_{\mathbf{p}}$ is decomposed by using a square root notation as follows

$$\Sigma_{\mathbf{p}} = \Sigma_{\mathbf{p}}^{1/2}\,\Sigma_{\mathbf{p}}^{1/2^T}, \tag{10}$$

where $\Sigma_{\mathbf{p}}^{1/2} \in \mathbf{R}^{n_p \times n_p}$ is the square root of $\Sigma_{\mathbf{p}}$, unique up to an orthogonal transformation of its columns[5]. With the help of the square root notation, the covariance between two stochastic quantities $\tilde{\mathbf{f}}, \tilde{\mathbf{g}} \in \{\tilde{\mathbf{A}}, \tilde{\mathbf{B}}, \tilde{\mathbf{E}}, \tilde{\mathbf{d}}_k\}$ can be decomposed as

$$\Sigma_{\mathbf{f},\mathbf{g}} = \mathbf{T_f}\,\Sigma_{\mathbf{p}}\,\mathbf{T_g}^T = \mathbf{T_f}\,\Sigma_{\mathbf{p}}^{1/2}\,\Sigma_{\mathbf{p}}^{1/2^T}\,\mathbf{T_g}^T = \Sigma_{\mathbf{f}}^r\,\Sigma_{\mathbf{g}}^{r\,T}. \tag{11}$$

Here, the more general notation $.^r$ is used to refer to the root form instead of $.^{1/2}$, since the matrices $\Sigma_{\mathbf{f}}^r$ and $\Sigma_{\mathbf{g}}^r$ are not necessarily square, and hence are not actual square roots of the considered matrices.

By applying the two manipulations discussed above to Equation (5), and by furthermore using following relation between the vectorization of a matrix and the Kronecker product[6] [49]

$$vec(\mathbf{AXB}^T) = (\mathbf{B} \otimes \mathbf{A})\,vec(\mathbf{X}) \tag{12}$$

the covariance $\Sigma_{\mathbf{x}_{k+1}}$ can be rewritten in square root form as follows

$$\begin{aligned}\Sigma_{\mathbf{x}_{k+1}}^r =& (\bar{\mathbf{x}}_k^T \otimes \mathbf{I}_{n_x})\Sigma_{\mathbf{A}}^r + \bar{\mathbf{A}}\,\Sigma_{\mathbf{x}_k}^r + (\mathbf{u}_k{}^T \otimes \mathbf{I}_{n_x})\Sigma_{\mathbf{B}}^r + \\ & (\bar{\mathbf{d}}_k^T \otimes \mathbf{I}_{n_x})\Sigma_{\mathbf{E}}^r + \bar{\mathbf{E}}\,\Sigma_{\mathbf{d}_k}^r.\end{aligned} \tag{13}$$

[5] Since the covariance matrix $\Sigma_{\mathbf{p}}$ is per definition a positive (semi-)definite matrix, this square root form can for example be obtained via the Cholesky factorization [48].

[6] More particularly, by using Equation (12), the product of a matrix $\mathbf{A}$ and a vector $\mathbf{x}$ can be rewritten as follows: $\mathbf{Ax} = vec(\mathbf{Ax}) = vec(\mathbf{IAx}) = (\mathbf{x}^T \otimes \mathbf{I})\,vec(\mathbf{A})$.

By using Equation (4) in combination with the square root form of the covariance, as presented by Equation (13), as the stochastic substitute for Equation (1a), the constraints are now linear in the optimization variables $\mathbf{u}_k$, $\bar{\mathbf{x}}_k$ and $\Sigma_{\mathbf{x}_k}^r$ (rather than $\Sigma_{\mathbf{x}_k}$), thereby guaranteeing the convexity of the problem.

Introducing uncertainties in the state constraints

By integrating the stochastic information in the state constraints, the hard state constraints (1b) and (1c) are transformed to chance constraints, as presented by Equation (14), which are the key characteristic of stochastic model predictive control formulation.

$$P(\tilde{\mathbf{x}}_k + \mathbf{s}_k \geq \mathbf{x}_k^{min}) \geq 1 - \epsilon_{\mathbf{x}_k} \quad \forall k \tag{14a}$$

$$P(\tilde{\mathbf{x}}_k - \mathbf{s}_k \leq \mathbf{x}_k^{max}) \geq 1 - \epsilon_{\mathbf{x}_k} \quad \forall k. \tag{14b}$$

Note that the slack variables $\mathbf{s}_k$ are retained to guarantee recursive feasibility under unbounded uncertainties [50].

The rationale behind chance constraints is the following. Since the open-loop stochastic OCP needs to decide upon an optimal control strategy before the actual values of the stochastic quantities are known, it tries to guarantee constraint satisfaction for possible realizations of the stochastic quantities in a probabilistic sense, by exploiting the knowledge of their distributions. The probability of constraint satisfaction is determined by the user-predefined risk-attitude $\{\epsilon_{\mathbf{x}_k}\}_{k=0\ldots K+1}$ (or risk-averseness level $1 - \epsilon_{\mathbf{x}_k}$), which enables a systematic trade-off between control performance and constraint satisfaction; $\epsilon \to 0$ corresponds to a very conservative attitude, whereas $\epsilon = 0.5$ reduces the chance constraints to their deterministic equivalent without any uncertainty anticipation [47, 51].

The constraint satisfaction can either be required for all inequality constraints altogether, over the whole prediction horizon K, resulting in joint chance constraints, or for every individual inequality constraint at each distinct time step, also referred to as individual chance constraints [50, 52–54]. Joint chance constraints typically become non-convex, for which an exact tractable representation might not exist [50], and hence are highly computationally intensive [52, 53]. Therefore, this work focuses on individual chance constraints.

Two main solution strategies have been adopted for chance constrained problems, being scenario-based

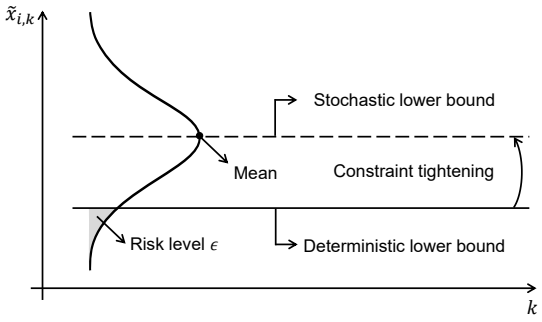


Figure 2: The visualization of the constraint tightening resulting from the analytical reformulation of chance constraints.

approaches and analytical approximation methods [50]. In scenario-based approaches, a properly chosen number of uncertainty realizations is describing the probability distributions, in order to obtain a finite number of sampled deterministic constraints replacing the original probabilistic constraints. Hence, scenario-based approaches, e.g., [15, 16, 20–22, 55–57], do not involve any assumption on the shape and support of the underlying probability distributions, but they can be computationally very demanding [15, 24, 50, 58]. Analytical approximation methods, on the other hand, directly reformulate the probabilistic constraints in deterministic terms. Consequently, they result in an OCP of similar complexity as the nominal, deterministic problem, thereby ensuring the tractability of the problem. However, this typically comes at the cost of some degree of conservativeness, due to the approximation(s) made [58, 59]. Nevertheless, for some specific probability distributions, such as Normal distributions, exact reformulations can be found [50, 59–61].

In this work, the analytical approximation method is pursued. According to this approach, chance constraints can be generally reformulated as deterministic ones by enforcing tightened constraints on the expected values of the states as visualized in Figure 2. If the marginal distributions of the different states $\tilde{x}_{i,k} = \mathbf{e}_i^T \, \tilde{\mathbf{x}}_k \; \forall i \in \mathbb{N}^{n_x}$ can be approximated as Normal distributions, the individual chance constraints can be equivalently (and exactly) reformulated as deterministic constraints as follows

$$\bar{x}_{i,k} + s_{i,k} \geq x_{i,k}^{min} + \Phi^{-1}(1-\epsilon_{x_{i,k}}) \sqrt{\Sigma_{x_{i,k}}^r \, {\Sigma_{x_{i,k}}^r}^T} \quad \forall i,k \tag{15a}$$

$$\bar{x}_{i,k} - s_{i,k} \leq x_{i,k}^{max} - \Phi^{-1}(1-\epsilon_{x_{i,k}}) \sqrt{\Sigma_{x_{i,k}}^r \, {\Sigma_{x_{i,k}}^r}^T} \quad \forall i,k \tag{15b}$$

where Φ^{-1} denotes the inverse Normal cumulative probability density function of $\tilde{x}_{i,k}$. The justification of using marginal Normal distributions in this work will be further discussed in Section 2.3.2.

The constraints (15a) and (15b) can be further recast to obtain efficiently solvable second-order cone constraints, by introducing an auxiliary optimization variable $\{\mathbf{q}_k \in \mathbb{R}^{n_x}\}_{k=0\ldots K+1}$

$$\bar{x}_{i,k} + s_{i,k} \geq x_{i,k}^{min} + \Phi^{-1}(1-\epsilon_{x_{i,k}}) \, q_{i,k} \quad \forall i,k \tag{16a}$$

$$\bar{x}_{i,k} - s_{i,k} \leq x_{i,k}^{max} - \Phi^{-1}(1-\epsilon_{x_{i,k}}) \, q_{i,k} \quad \forall i,k \tag{16b}$$

$$q_{i,k} \geq \|\Sigma_{x_{i,k}}^r\|_2 \quad \forall i,k \tag{16c}$$

where the first two constraints define a half space in the optimization variables and the last constraint defines a second-order cone, which all together define a convex set.

The combination of Equations (16a) - (16c) replaces Equations (1b) and (1c) in the stochastic OCP formulation.

Introducing uncertainties in the input constraints

For the input constraints it is recommended to introduce affine disturbance feedback, to reduce conservatism [17,19,24,52,62]. Following this approach, the control inputs are reformulated as an affine function of the preceding uncertainty manifestations, thereby mimicking the closed-loop behavior of MPC in the open-loop control problem [17, 19, 24, 47, 50, 52, 62]. Using the previously introduced notation, this can be

written as follows.

$$\begin{aligned}\mathbf{u} \rightarrow \tilde{\mathbf{u}} &= \bar{\mathbf{u}} + \delta\mathbf{u} \\ \text{with } \tilde{\mathbf{u}} &= [\tilde{\mathbf{u}}_0^T \,...\, \tilde{\mathbf{u}}_k^T \,...\, \tilde{\mathbf{u}}_K^T]^T \\ \bar{\mathbf{u}} &= \mathbb{E}[\tilde{\mathbf{u}}] \\ \Sigma_{\mathbf{u}} &= \mathbb{E}[\delta\mathbf{u}\,\delta\mathbf{u}^T] = \mathbf{T_u}\,\Sigma_{\mathbf{p}}\,\mathbf{T_u}^T \end{aligned} \tag{17}$$

Note that the inputs are rewritten in the same way as the stochastic quantities in Equations (2) and (8). However, the important difference is that the mean $\bar{\mathbf{u}}$ as well as the selection matrix $\mathbf{T_u}$ are now optimization variables, rather than fixed, predefined parameters. The selection matrix $\mathbf{T_u}$ should be interpreted as a feedback gain matrix, that guarantees causality by ensuring that the control input at time step k can only react to the uncertainty manifestations up to time $k-1$. Also note that the first control input is not a function of any uncertainty, since it is assumed that at the first time step, the currently prevailing states and inputs are known [24, 50].

Since the inputs now also become functions of stochastic random variables, the input constraints (1e) are replaced by chance constraints on the individual inputs $\tilde{u}_{j,k} = \mathbf{e_j}^T\,\tilde{\mathbf{u}}_k \;\forall j \in \mathbb{N}^{n_u}$, similarly to Equation (16). However, in contrast to the thermal comfort requirements, the input constraints cannot just be violated, since they represent restrictive technical system limits. Hence, small values need to be assigned to $\epsilon_{\mathbf{u}_k}$, so that the original requirements are met with a high probability [24, 62]. Because of the structure of $\mathbf{T_u}$, the reformulation of the input constraints has nevertheless no impact on the constraints imposed for the first time step, which still remain hard constraints. As such, when implementing the MPC strategy in closed-loop, the technical system limits will never be actually violated [24].

The introduction of ADF requires a slight adaptation to the structure of the latent variable $\tilde{\mathbf{p}}$. To allow for a proper reaction against the uncertainty realizations in Equation (17) via the feedback gain matrix $\mathbf{T_u}$, it should be made explicit that the model uncertainties persist, and thus reoccur every single time step. Hence, they should be repeated in $\tilde{\mathbf{p}}$, $\bar{\mathbf{p}}$ and $\Sigma_{\mathbf{p}}$. This adaptation leads to the covariance presented by Equation (18). Note that the covariance of the state space matrices $\tilde{\mathbf{A}}, \tilde{\mathbf{B}}$ and $\tilde{\mathbf{E}}$ on the one hand, and of the disturbances $\{\mathbf{d}_k\}_{k=0\ldots K}$ on the other hand, are grouped into a larger covariance matrix, to account for possible correlations between their elements.

$$\Sigma_{\mathbf{p}} = \left[\begin{array}{cccc|c} \Sigma_{\mathbf{A},\mathbf{B},\mathbf{E}} & \mathbf{0} & \cdots & \mathbf{0} & \\ \mathbf{0} & \Sigma_{\mathbf{A},\mathbf{B},\mathbf{E}} & \cdots & \mathbf{0} & \mathbf{0} \\ \vdots & \vdots & \ddots & \vdots & \\ \mathbf{0} & \mathbf{0} & \cdots & \Sigma_{\mathbf{A},\mathbf{B},\mathbf{E}} & \\ \hline \multicolumn{4}{c|}{\mathbf{0}} & \Sigma_{\{\mathbf{d}_k\}_{k=0\ldots K}} \end{array}\right] \tag{18}$$

The structure of the associated feedback gain matrix $\mathbf{T_u}$, consisting of two strictly lower block triangular matrices, is represented by Equation (19); here, the dots $\bullet$ indicate the non-zero sub-matrices.

$$\mathbf{T_u} = \left[\begin{array}{cccc|cccc} \mathbf{0} & \mathbf{0} & \cdots & \mathbf{0} & \mathbf{0} & \mathbf{0} & \cdots & \mathbf{0} \\ \bullet & \mathbf{0} & \cdots & \mathbf{0} & \bullet & \mathbf{0} & \cdots & \mathbf{0} \\ \vdots & \vdots & \ddots & \vdots & \vdots & \vdots & \ddots & \vdots \\ \bullet & \cdots & \bullet & \mathbf{0} & \bullet & \cdots & \bullet & \mathbf{0} \end{array}\right] \tag{19}$$

Finally, since the inputs $\mathbf{u}_k$ are no longer considered in their deterministic form, the previously derived formulation for the covariance of the states, as presented by Equation (13), needs to be altered, leading to

$$\begin{aligned}\Sigma^r_{\mathbf{x}_{k+1}} =& (\bar{\mathbf{x}}_k^T \otimes \mathbf{I}_{n_x})\Sigma^r_{\mathbf{A}} + \bar{\mathbf{A}}\,\Sigma^r_{\mathbf{x}_k} + \\ & (\bar{\mathbf{u}}_k^T \otimes \mathbf{I}_{n_x})\Sigma^r_{\mathbf{B}} + \bar{\mathbf{B}}\,\Sigma^r_{\mathbf{u}_k} + \\ & (\bar{\mathbf{d}}_k^T \otimes \mathbf{I}_{n_x})\Sigma^r_{\mathbf{E}} + \bar{\mathbf{E}}\,\Sigma^r_{\mathbf{d}_k}. \end{aligned} \tag{20}$$

Resulting stochastic OCP formulation

Combining all previously introduced steps, the following stochastic OCP formulation, explicitly accounting for both additive and parametric uncertainties, is obtained

$$\min_{\rtimes} \phi\,(\rtimes) \tag{21a}$$

subject to

$$\begin{aligned} \bar{\mathbf{x}}_{k+1} &= \bar{\mathbf{A}}\,\bar{\mathbf{x}}_k + \bar{\mathbf{B}}\,\mathbf{u}_k + \bar{\mathbf{E}}\,\bar{\mathbf{d}}_k \qquad \forall k \\ \Sigma^r_{\mathbf{x}_{k+1}} &= (\bar{\mathbf{x}}_k^T \otimes \mathbf{I}_{n_x})\Sigma^r_{\mathbf{A}} + \bar{\mathbf{A}}\,\Sigma^r_{\mathbf{x}_k} + \\ & \quad (\bar{\mathbf{u}}_k^T \otimes \mathbf{I}_{n_x})\Sigma^r_{\mathbf{B}} + \bar{\mathbf{B}}\,\Sigma^r_{\mathbf{u}_k} + \\ & \quad (\bar{\mathbf{d}}_k^T \otimes \mathbf{I}_{n_x})\Sigma^r_{\mathbf{E}} + \bar{\mathbf{E}}\,\Sigma^r_{\mathbf{d}_k} \qquad \forall k \end{aligned}$$

$$
\begin{aligned}
\bar{x}_{i,k} + s_{i,k} \geq\ & x_{i,k}^{min} + \Phi^{-1}(1-\epsilon_{x_{i,k}})\, q_{i,k} && \forall i,k \\
\bar{x}_{i,k} - s_{i,k} \leq\ & x_{i,k}^{max} - \Phi^{-1}(1-\epsilon_{x_{i,k}})\, q_{i,k} && \forall i,k \\
& q_{i,k} \geq \|\Sigma^r_{x_{i,k}}\|_2 && \forall i,k \\
& s_{i,k} \geq 0 && \forall i,k \\
\bar{u}_{j,k} + t_{j,k} \geq\ & \mathbf{0}_{n_u} + \Phi^{-1}(1-\epsilon_{u_{j,k}})\, r_{j,k} && \forall j,k \\
\bar{u}_{j,k} - t_{j,k} \leq\ & u_{j,k}^{max} - \Phi^{-1}(1-\epsilon_{u_{j,k}})\, r_{j,k} && \forall j,k \\
& r_{j,k} \geq \|\Sigma^r_{u_{j,k}}\|_2 && \forall j,k \\
& \Sigma^r_{\mathbf{u}} = \mathbf{T_u}\, \Sigma^r_{\mathbf{p}} && \\
& t_{j,k} \geq 0 && \forall j,k \\
& \mathbf{x}(0) = \mathbf{x}_0 && \\
& \mathbf{u}(0) = \mathbf{u}_0 && \\
& && \text{(21b)}
\end{aligned}
$$

with

$$
\begin{aligned}
\rtimes = \{ & \{\bar{\mathbf{x}}_k\}_{k=0\ldots K+1}, \{\Sigma^r_{\mathbf{x}_k}\}_{k=0\ldots K+1}, \\
& \{\mathbf{q}_k\}_{k=0\ldots K+1}, \{\mathbf{s}_k\}_{k=0\ldots K+1} \\
& \{\bar{\mathbf{u}}_k\}_{k=0\ldots K}, \mathbf{T_u}, \\
& \{\mathbf{r}_k\}_{k=0\ldots K}, \{\mathbf{t}_k\}_{k=0\ldots K}\} \qquad \text{(21c)}
\end{aligned}
$$

Since only linear constraints and second-order cone constraints are added compared to the convex, deterministic OCP (1), the derived stochastic OCP (21) remains convex if $\phi(\rtimes)$ is convex in $\rtimes$.

2.3.2 Uncertainty characterization

The mathematical model of the uncertainties is an essential part of the stochastic OCP formulation derived above. This section further elaborates on how the different stochastic quantities $\tilde{\mathbf{A}}, \tilde{\mathbf{B}}, \tilde{\mathbf{E}}$ and $\tilde{\mathbf{d}}_k$ can be properly represented by their mean and covariance, delineating the underlying probability density functions.

Since the exact controller model structure determines which specific form $\tilde{\mathbf{A}}, \tilde{\mathbf{B}}, \tilde{\mathbf{E}}$ and $\tilde{\mathbf{d}}_k$ take, the model structure first needs to be imposed, before proceeding with the uncertainty characterization.

System model specification

Due to the fact that the mathematical complexity (i.e., the number of optimization variables and constraints) of the stochastic OCP (21) highly depends on the order of the building controller model, because of the repetition of the parametric uncertainty in the latent variable $\tilde{\mathbf{p}}$ (see Equation (18)), a reduced order model of sufficiently low order is preferred. Model orders as low as two or three are shown to be sufficient to adequately represent the general heat dynamics of buildings [5, 63–66]. In this work, based on the findings of Reynders et al [63, 67], a building model of order four is used, which is shown in Figure 3. This model uses an electric circuit analogy, introducing resistances (R) and capacitances (C), to represent a residential dwelling. It serves as a good compromise between complexity and interpretability, since it is of sufficiently low order, but still distinguishes between all fundamentally different construction elements and boundary conditions[7]. The model approximates the building as one thermal zone, represented by four states, being the indoor air, T_i, external walls, T_w, internal walls, T_{wi}, and floor, T_f. An additional state is considered for the low-temperature radiator system, T_{rad}, which is assumed to be ideal, with a 100% ef-

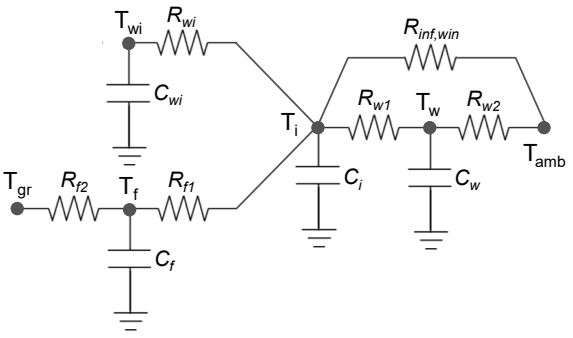


Figure 3: The model structure of the reduced order RC model, where a residential building is modeled as one thermal zone, represented by four states. The heat inputs, either the heat emitted by the radiators, the solar heat gains, or the internal heat gains, are not shown; they are all distributed over the capacities of the different states in proportion to their surface area, relative to the total surface area of all building construction elements, by using distribution coefficients. Adapted from [67].

[7] The considered theoretical, reduced order white-box building model entails one important assumption that may limit practical implementation (not limiting in the simulations), being that direct measurements of the internal heat gains are available, which are in practice difficult to obtain. An alternative approach would be to use the domestic electricity use, available from digital/smart meter data, as an alternative input to construct a data-driven, grey-box building model, as is for example suggested by Reynders et al. [63].

ficiency. The heat delivered to the radiators is coming from a single heat supply system[8], $\dot{Q}_{sup}$, and is assumed to be a heat pump in this work. The system is subject to seven disturbances, being the ambient temperature, T_{amb}, the ground temperature, T_{gr}, the solar heat gains along the four cardinal directions, $\dot{Q}_{solN}, \dot{Q}_{solE}, \dot{Q}_{solS}$ and $\dot{Q}_{solW}$, and the internal heat gains from the occupants, $\dot{Q}_{int}$. Hence, $\tilde{\mathbf{x}}_k$, $\tilde{\mathbf{u}}_k$ and $\tilde{\mathbf{d}}_k$ take the following form in this work

$$\tilde{\mathbf{x}}_k = \begin{bmatrix} \tilde{T}_{i,k} \\ \tilde{T}_{w,k} \\ \tilde{T}_{wi,k} \\ \tilde{T}_{f,k} \\ \tilde{T}_{rad,k} \end{bmatrix}, \tilde{\mathbf{u}}_k = \begin{bmatrix} \tilde{\dot{Q}}_{sup,k} \end{bmatrix}, \tilde{\mathbf{d}}_k = \begin{bmatrix} \tilde{T}_{amb,k} \\ \tilde{T}_{gr,k} \\ \tilde{\dot{Q}}_{solN,k} \\ \tilde{\dot{Q}}_{solE,k} \\ \tilde{\dot{Q}}_{solS,k} \\ \tilde{\dot{Q}}_{solW,k} \end{bmatrix}; \tag{22}$$

the state space matrices are defined accordingly.

Building model parameter uncertainty

The values of the (uncertain) building model parameters can either be obtained via a physics-based [66, 68, 69] or via a data-driven [63, 64, 69] approach. In order to include domain knowledge and thus maximize insight, this work adopts a physics-based approach, that links the stochasticity of the parameters of a reduced order white-box model to the underlying uncertainty of the physical properties. It should be stressed that this choice does not detract from the more general applicability of the proposed stochastic OCP formulation. Indeed, also data-driven modeling approaches, such as grey-box modeling, result in uncertain parameter estimations [70], which can be characterized by a covariance matrix [71], and as such, can be directly incorporated in the proposed SMPC approach.

The stochasticity of the parameters of a physics-based building controller model is caused by a lack of knowledge about the building envelope. Since the building geometry and construction year can often be derived from the building address based on geographic information systems data and cadastral data, the uncertainties can be mainly attributed to the building thermal properties [43]. De Jaeger et. al [42, 43] developed a statistical, data-driven building characterization method that leverages governmental databases of the energy performance of buildings to obtain probability distributions, as well as correlated samples, of the U-values of the ground floor, external walls, windows and roof and of the window-to-wall ratio for a particular dwelling. Building further upon this work, a substantiated estimate of the parametric uncertainty of the building controller model can be obtained. This approach was investigated in detail in our previous research[9] [72]. The obtained correlated samples and probability distributions of the R and C parameters in [72], representing all possible dwelling realizations, still need to be converted into a statistical description of the discrete-time state space matrices, in terms of their mean and covariance, in order to incorporate them in the stochastic OCP formulation. Since the SSM elements $\{a_{i,j}\}_{i,j=1\ldots n_x}, \{b_{i,k}\}_{i=1\ldots n_x, k=1\ldots n_u}$ and $\{e_{i,l}\}_{i=1\ldots n_x, l=1\ldots n_d}$, which can be directly derived from the R and C parameters, closely approximate a Normal distribution, these parameters are used to build up $\tilde{\mathbf{p}}$. The covariance $\Sigma_{\mathbf{A},\mathbf{B},\mathbf{E}}$ can be straightforwardly determined by considering all samples of all SSM elements altogether. To capture the correlation between the different SSM elements, the average state space matrices $\bar{\mathbf{A}}, \bar{\mathbf{B}}$ and $\bar{\mathbf{E}}$ are replaced by reference state space matrices $\bar{\bar{\mathbf{A}}}, \bar{\bar{\mathbf{B}}}$ and $\bar{\bar{\mathbf{E}}}$, which closely approximate the average model, but also respect the actual dynamics. The reference SSM is determined by selecting the sampled SSM $\mathbf{z}_s \ni \{\mathbf{A}_s, \mathbf{B}_s, \mathbf{E}_s\}$ that has the lowest weighted distance to the average model $\bar{\mathbf{z}}$, where this weighted distance to the mean (WDM) for a particular sample s is defined as

$$WDM_s = (\mathbf{z}_s - \bar{\mathbf{z}})^T \Sigma_{\mathbf{z}}^{-1} (\mathbf{z}_s - \bar{\mathbf{z}}), \tag{23a}$$

with

$$\mathbf{z}_s = \begin{bmatrix} vec(\mathbf{A}_s) \\ vec(\mathbf{B}_s) \\ vec(\mathbf{E}_s) \end{bmatrix}, \bar{\mathbf{z}} = \begin{bmatrix} vec(\bar{\mathbf{A}}) \\ vec(\bar{\mathbf{B}}) \\ vec(\bar{\mathbf{E}}) \end{bmatrix}, \Sigma_{\mathbf{z}} = cov(\tilde{\mathbf{z}}, \tilde{\mathbf{z}}). \tag{23b}$$

This weighting is needed to account for the fact that different state space elements - even within the same state space matrix - can have very different dimensions.

[8] Since only one heat input is considered, the index j is omitted from now on.

[9] In [72], an RC model of order nine is considered. In this work, the model order is further reduced to an order of four, to ensure that the optimization problem remains tractable, given the repetition of the parametric uncertainty in the latent variable $\tilde{\mathbf{p}}$.

Weather forecast uncertainty
In contrast to the building model parameters, there is a clear consensus on how to model the weather forecast uncertainty, covering the ambient temperature and solar heat gains[10], since it is unequivocally defined by the difference between the forecast and the actual weather conditions.

Lambrichts [73] compared the actual weather conditions recorded at the Vliet test building of the KU Leuven Laboratory of Building Physics, located in Leuven (Belgium), with the corresponding weather forecasts made by the Royal Belgian Meteorological Institute (RMI). The forecast errors collected by Lambrichts are further processed in this work, in order to come up with an accurate characterization of the weather forecast uncertainty. The forecast errors are split up in different datasets according to the moment of the day when the forecast is made, so that this impact on the forecast uncertainty can be taken into account. Besides, within one dataset, an explicit distinction is being made between forecasts made for different look-ahead times, thereby acknowledging that the uncertainty is likely to increase with an increasing forecast horizon. Since the RMI provides forecasts with a prediction horizon of 60 h, which are being updated every 6 h, four different datasets are distinguished, each containing 60 h-forecasts for both the ambient temperature and solar heat gains. Each of these datasets is used to characterize the probability distributions of the weather forecast errors in terms of their (time-dependent) mean and covariance (accounting for both the auto-correlation and cross-correlation). This information is subsequently used to constitute $\bar{\mathbf{d}}_k$ and $\Sigma^r_{\mathbf{d}_k}$, which will take different forms depending on the moment of the day when the OCP is being solved, and on the considered optimization horizon.

As a final remark, it should be stressed that the mean value $\bar{\mathbf{d}}_k$ is determined by a reverse engineering approach, by generating correlated samples from the forecast error distributions, and by subsequently subtracting them from the available measurement data at the Vliet test building. Although this reverse engineering approach obviously would not work in real-life applications requiring dedicated forecast algorithms, it suffices for the theoretical setting considered here to illustrate the functionality of the SMPC approach under discrepancies between forecasts and actual data.

Occupant behavior forecast uncertainty
The uncertainty on the occupant-related disturbance forecasts, covering the internal heat gains, is complicated due to the complex stochastic nature of human behavior, which is determined by many personal factors [74]. Dedicated approaches can be found in literature, implementing rigorous occupancy models combined with real-time, on-site measurements. This is for example done by Mady et al. [75], who implemented a stochastic occupancy model based on Markov chains as an input of an MPC algorithm, where the computation of the occupancy sequence is revisted at every time step. Another valuable approach is the learning-based approach, see e.g., [55], where the statistics of the uncertainties are continuously and dynamically inferred from real data.

Although the development of detailed occupancy forecast models is out-of-scope of this paper, the working principle of such an approach can be imitated via a workaround as follows. With the help of the open web tool StROBe (Stochastic Residential Occupancy Behaviour)[11] [76], an explicit occupancy modeling toolbox developed at the KU Leuven Building Physics Section, a yearly profile for the internal heat gains can be generated. This yearly profile is considered as a proxy for an actually measured profile, and is subsequently used to determine an average daily profile and associated variance. The average daily profile can then be used as a forecast for the internal heat gains (with a zero mean forecast error), and as such can be directly incorporated in $\bar{\mathbf{d}}_k$; the (square root of the) variance, on the other hand, can be used to constitute $\Sigma^r_{\mathbf{d}_k}$.

The temperature setpoints are assumed to be deterministic, and hence, fixed and known in this work. This is motivated by the findings of Guerra et al. [74], who observed that in dwellings with programmable thermostats, occupants take fewer deliberate actions,

[10] The uncertainty on the ground temperature is not considered in this work, since the forecasts and actual measurement data required for a proper uncertainty characterization are hard to obtain [73]. In fact, the temporal variation of the ground temperature is not even considered, as argued in [63], since it is unrealistic that local measurements can be actually used as an input to the building controller model; rather, a constant value of 10 °C is used.

[11] Note that in this work, an updated StROBe version is used, extended by Jansen, to include the metabolic heat rates in addition to the heat gains caused by appliances and lighting; see `https://github.com/jelgerjansen/StROBe/tree/output_occupancy_profiles`

and leave the control to the thermostat. Nevertheless, if desired, the uncertainty on the setpoints can be straightforwardly included by also writing $\mathbf{x}_{min}^k$ and $\mathbf{x}_{max}^k$ as stochastic quantities in Equation (14), and by treating $\tilde{\mathbf{x}}_k^* = \tilde{\mathbf{x}}_k - \tilde{\mathbf{x}}_{min}^k$ or $\tilde{\mathbf{x}}_k^* = \tilde{\mathbf{x}}_k - \tilde{\mathbf{x}}_{max}^k$ (rather than $\tilde{\mathbf{x}}_k$) as a stochastic variable in the elaboration discussed in Section 2.3.1.

Now that all relevant uncertainties are properly characterized, the development of the SMPC strategy is complete. The next important step is to assess its performance, and appraise its potential added value compared to currently prevailing MPC strategies.

2.4 SMPC performance assessment

To properly appraise the potential added value of the proposed SMPC^{ap} strategy, its performance is assessed in the context of both optimal control and optimal design, by considering two case studies.

The performance assessment is done based on two performance metrics, being the thermal comfort violations (TCV), and the specific thermal energy demand (TED). The thermal comfort is determined by the condition of the state representing the indoor air temperature $x_{i,k} = T_{i,k}$[12,13]. The total energy demand is in turn determined by the heat input delivered by the heat supply system, expressed relative to the net floor area of the building.

$$TCV = \sum_{k=0\dots K} max(x_{i,k}^{min} - \bar{x}_{i,k}, 0)\Delta t \tag{24}$$

$$TED = \sum_{k=0\dots K} \frac{\bar{u}_k \Delta t}{A_{floor}} \tag{25}$$

2.4.1 Optimal control performance assessment

To investigate the effectiveness of the proposed SMPC^{ap} strategy for optimal building climate control under uncertainty, its performance is compared to the following control strategies:

- **Performance bound (PB) MPC** PBMPC assumes perfect knowledge of the system dynamics and future disturbance realizations in the OCP, i.e., the uncertainty is absent and the stochastic quantities are equal to their actual, future values. Hence, the system is not subject to closed-loop perturbations. This is not a controller, but rather a theoretical concept, which can serve as a benchmark for other control strategies; it illustrates the best possible (but not actually attainable) MPC performance.

- **Deterministic (D) MPC** DMPC, also known as certainty equivalence MPC, considers the deterministic OCP formulation (1) without uncertainty anticipation, i.e., the chance constraints are solved for $\epsilon = 0.5$, and all predictions are assumed to be correct (i.e., equal to certain). Uncertainties are nevertheless present in the closed-loop simulations, causing the actual model parameters and disturbances to differ from the nominal values assumed in the OCP. This strategy follows common practice.

- **Stochastic MPC** SMPC explicitly accounts for the uncertainties in the OCP formulation (21), in order to limit the detrimental impact of the closed-loop perturbations. A distinction is being made between SMPC only accounting for additive (disturbance forecast) uncertainty, SMPC^{a}, which is the current state-of-the-art strategy for building climate control, and SMPC taking into account both additive and parametric (model) uncertainty, SMPC^{ap}, corresponding to the proposed novel strategy.

The difference in information used by the different controllers in the OCP formulation is summarized in Table 1.

To assess the control performance, all MPC strategies are implemented in closed-loop, using a receding horizon, as illustrated in Figure 1. Since no model-structure uncertainty is considered, the emulator model representing the actual system, and used for the state updates, is characterized by the same model equations, but different model parameters, as

[12] In this work, thermal comfort is assessed based on the state of the air thermal capacity of the building model, instead of on the operative temperature (which is typically used in comfort standards [77]), since the radiative temperatures of the surrounding building components are not explicitly considered in the chosen building model.

[13] Because of the particular setting considered in this paper, focusing on optimal space heating at minimal energy use, the controller is compelled to stick to the lower temperature bound, implying that the upper temperature bound is of minor importance here.

Table 1: The information used in the OCP formulation by the different considered MPC strategies.

		actual value	mean/ref. value	covariance
PBMPC	weather forecast	x		
	occ. beh. forecast	x		
	building model	x		
DMPC	weather forecast		x	
	occ. beh. forecast		x	
	building model		x	
SMPC[a]	weather forecast		x	x
	occ. beh. forecast		x	x
	building model		x	
SMPC[ap]	weather forecast		x	x
	occ. beh. forecast		x	x
	building model		x	x

the controller model used in the OCP formulation (except for the PBMPC strategy, where the controller and emulator model are equal). Perfect state updates and full state information are assumed, to avoid additional interference of noise introduced by a state estimator. Thereby, the impact of measurement errors, system errors, and the like are ruled out. For the state updates, all controllers use the same information, being the actual building model parameters, the actual weather realizations and the actual internal heat gain realizations.

In this work, more particularly, the TCV and TED of the different MPC strategies are evaluated by simulations for a residential dwelling for one week, during the first seven days of January. All controllers pursue an energy use minimization, and consider a time step of $1\,\mathrm{h}$ and an optimization horizon of $60\,\mathrm{h}$, restricted by the characteristics of the available disturbance forecasts. For the SMPC approaches, different risk levels ($\epsilon = 0.6 \rightarrow 0.999$) are considered, in order to fully cover their possible operating region.

The considered residential building in this study is selected from the set of dwellings for which the parametric uncertainty is studied in detail in our previous research [72]. Here, the terraced, small, older (but renovated) heavy-weight dwelling is considered. The most important characteristics are summarized in Table 2.

Table 2: The most important characteristics regarding construction year (known), geometry (known) and thermal quality (uncertain) of the studied building.

Construction year [-]	<1950
Detachment level [-]	terraced
Net floor area [m²]	129
Protected volume [m³]	406
Ground floor area [m²]	87
Façade area [m²]	80
Roof area [m²]	95
UA building [W/K]	130-668

For more information about the building characteristics, and the probability distribution of the U-values of the construction elements, as well as of the R and C parameters, the reader is referred to [72]. The controller model used to represent this building in the OCP formulation, as explained in Section 2.3.2, is either the reference SSM (in case of DMPC, SMPC[a] or SMPC[ap]), possibly combined with the corresponding covariance matrix, or the emulator model (in case of PBMPC), where the emulator model corresponds to a sampled SSM. To maximize insight, the performance assessment considers different emulator models, representing different cases of model uncertainty. Seven different SSMs, each representing a possible realization of the studied building, are selected from the total set of 100 possible building models obtained in [72]. The first one is the reference, with the smallest WDM (Equation (23)); this in fact corresponds to the case without model uncertainty. Then, two building samples with a moderate WDM are selected, one with a smaller nominal heat demand[14] than the reference building, and one with a larger one. The same is done for two building samples with a large WDM. Finally, also the building samples with the overall smallest and largest nominal heat demand are included, so that also the 'worst case' and 'best case' possible building realizations are considered in the analysis. The characteristics of the seven considered building realizations, covering the whole range of possible realizations of the studies building in a systematic way, are summarized in Table 3.

[14] The nominal heat demand is quantified following NBN EN 12831, considering an extremely cold day (according to the Belgian climate) with an outside temperature of −8 °C, a ground temperature of 10 °C, and an indoor temperature of 20 °C [78].

Table 3: The most important characteristics distinguishing the seven considered realizations of the studied building.
Rather than mentioning the actual WDM value, the WDM is represented by an index, ranging from 1 for the reference building, to 100 for the realization that differs the most from the reference.

sample	$\dot{Q}_{nom}$ [W]	WDM index [-]	UA [W/K]
A	4080 (min)	81	130
B	6334	95	214
C	8582	50	360
REF	9033	1	295
D	11996	53	457
E	11303	100	480
F	14959 (max)	96	668

The maximum thermal power bound to be used as a constraint in the OCP formulation is determined by the capacity of the heat supply system in place, which is assumed to be sized according to the nominal heat demand of the building. In case model uncertainty is being considered (i.e., in all cases except for PBMPC), the sizing is done based on the reference model and takes into account a safety factor of 1.5, in order to acknowledge that there may exist a significant discrepancy between the reference model and real-world[15].

For the actual ambient temperature and solar heat gains realizations, measurement data of the year 2016 are used, recorded at the Vliet test building of the KU Leuven Laboratory of Building Physics, located in Leuven (Belgium). For the actual internal heat gain realizations, a StROBe profile of a 4-persons-household, consisting of two full-time employed adults and two school-age children, is used. As explained in Section 2.3.2, the thermal comfort requirements are considered to be fixed. In this study, a minimum temperature of 20 °C is requested during daytime (i.e., 07:00 - 23:00), combined with a night setback of 16 °C. The maximum allowed temperature is set to 28 °C[16].

[15] The point of view adopted in this paper differs from the one adopted in current practice, where one typically assumes that a sufficiently accurate building model is available. To account for the impact of the significant parametric uncertainty in this work, a high safety factor is used on top of the worst-case static design conditions.

[16] The upper thermal comfort bound is of minor importance in this work, since the controller will try to stick to the lower temperature bound as it tries to minimize the energy use.

The expected value and covariance of the disturbance forecasts are derived by applying the methods described in Section 2.3.2. Since the proposed uncertainty characterization method for the occupant behavior forecast is not underpinned by actual data[17], and turns out to result in a very large variance, the control performance assessment is done twice, one time with and one time without uncertainty on the internal heat gains. By considering these two cases, the impact of the balance between the additive and parametric uncertainty is taken into account, allowing for a more nuanced view on the added value of the SMPC^{ap} strategy.

2.4.2 Optimal design performance assessment

The main goal of the second case study is to illustrate the potential of an integrated optimal control and design approach and the added value of considering parametric and additive uncertainties therein.

Rather than fully implementing a nested design-control optimization, which is out of scope of this work, the outer optimization loop steering the design decisions is replaced by a set of predetermined design scenarios, focusing on high-level decisions regarding the size of the heat supply system. For the lower-level control loop, the same MPC approaches are compared as in the previous case study, being PBMPC, DMPC, SMPC^{a} and SMPC^{ap}, all minimizing the overall energy use. PBMPC, or any other open-loop deterministic alternative, can be considered as the current practice in an IOCD context: it considers the dynamic system behavior in a predefined setting, for a postulated set of boundary conditions. Due to the negligence of uncertainties, this approach is likely to result in a too strictly (under)sized system. To correct for this, a closed-loop approach should rather be considered, where the impact of the perturbations is taken into account when making a design decision. This can be considered as the dynamic equivalent of the safety factor used in static design methods. Here, both DMPC and SMPC are looked at.

To assess and compare the suitability of the different control strategies to be used in an optimal design context (and to investigate the potential added value of using the SMPC^{ap} approach), the most ap-

[17] In contrast to the uncertainty characterization of the building model parameters and weather forecasts, wich are both based on a rigorous and extensive data-analysis.

propriate heat supply system size for each of the four control strategies is determined via a simplified IOCD application, and subsequently compared, as follows. Given a particular installed thermal power (design decision), and a particular risk-averseness level (control decision) ($1-\epsilon = 0.5$ for PBMPC and DMPC, or $0.5 < 1-\epsilon < 0.999$ for SMPC^{a} or SMPC^{ap}), the chosen MPC approach is applied, after which the resulting thermal discomfort is determined. This is done for different building samples (i.e., emulator models), resulting in a thermal discomfort range, rather than one single value for the thermal discomfort to be expected for a particular dwelling. This procedure is repeated for different heat supply sizes, and risk-averseness levels (as far as the SMPC approaches are concerned), resulting in a whole set of thermal discomfort ranges, that can be used to make proper design decisions. For every MPC strategy, the heat production capacity is then selected that guarantees the lowest (preferably zero) thermal discomfort range for all considered building samples.

The whole evaluation is again simulation-based. Ideally, the optimal control part should be run for a full-year, or at least for a set of representative days, in order to make sure that the different operating regimes that the system might encounter, are sufficiently covered [34]. However, since this is only an exploratory case study, the evaluation is restricted to one day, where challenging weather conditions according to the Belgian climate apply. Here, the 18th of January 2016 is chosen, characterized by temperatures that are well below zero throughout the entire day. Apart from the altered weather conditions and maximum thermal power bounds, the simulation set-up is equal to that of the first case study, in terms of considered building samples and occupant behavior.

3 Results and discussion

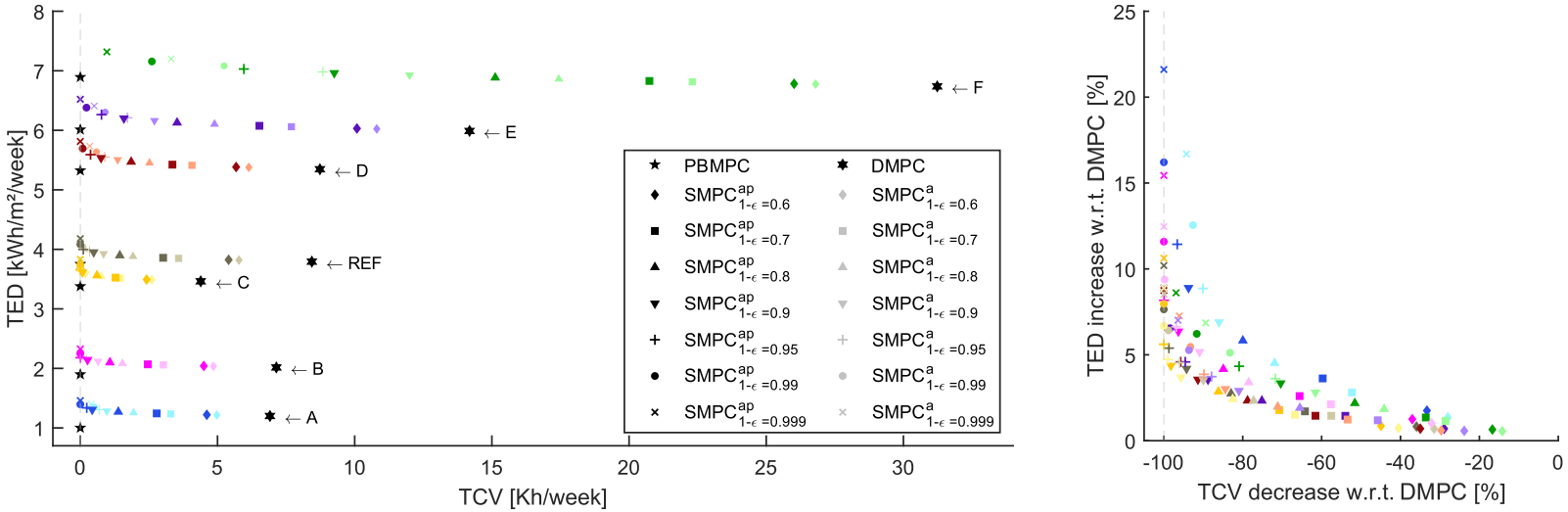
In this section, the results of the case studies presented in Section 2.4 are discussed, aiming at illustrating the added value of the proposed SMPC^{ap} approach compared to the state-of-the-art. Section 3.1 focuses on the attainable thermal comfort improvement by hedging against additive as well as parametric uncertainties in an optimal control context, and on the related energy costs. Section 3.2 discusses the potential of an integrated optimal control and design methodology incorporating the SMPC^{ap} strategy to obtain a more appropriate, yet robust, sizing of the heat supply system.

3.1 Optimal control performance assessment

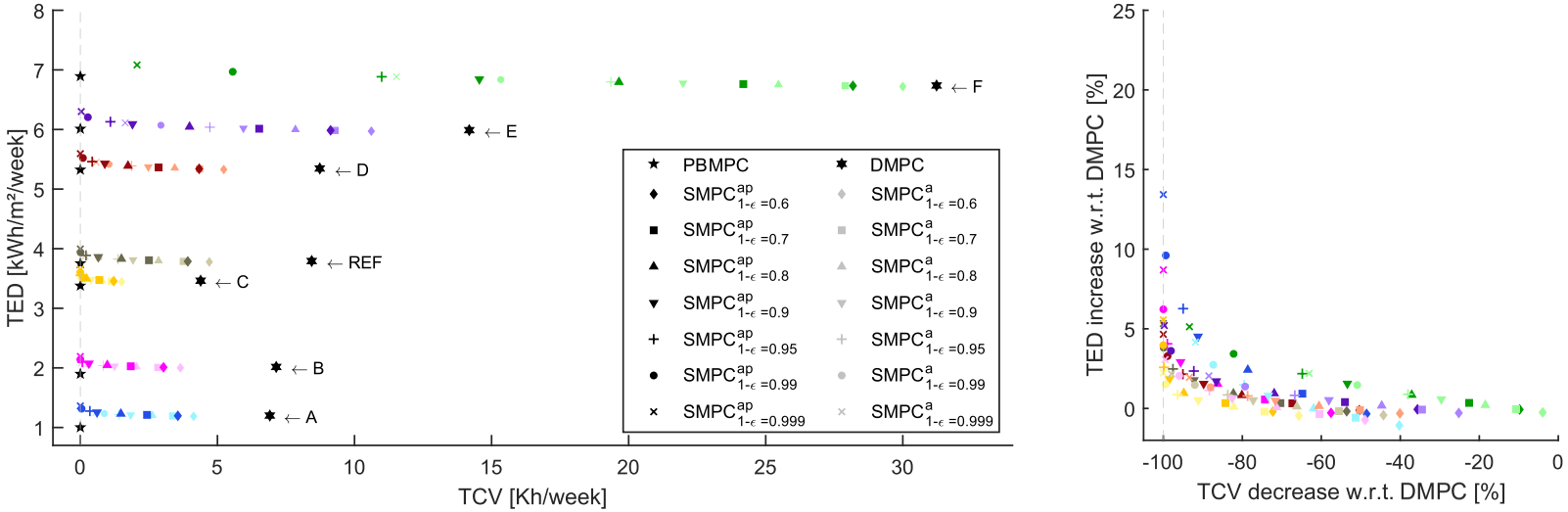
As we will illustrate below, the SMPC^{ap} approach yields thermal comfort improvements at the expense of limited increases in energy use. These gains are most prominent in buildings characterized by the combination of a large model uncertainty and a large nominal heat demand, and this at a limited cost.

Figure 4 summarizes the performance, in terms of thermal comfort violations and specific thermal energy demand, of the PBMPC, DMPC, SMPC^{a} and SMPC^{ap} strategies, for the first week of January 2016. For each considered realization of the studied building, the figure visualizes i) the best case (theoretical) control performance of the PBMPC strategy (★), guaranteeing no thermal comfort violations (TCV = 0) at the lowest energy use, ii) the worst case control performance of the DMPC strategy (✶), and iii) the intermediate control performance of the SMPC^{a} and SMPC^{ap} strategies, subject to a trade-off between TCV and TED, depending on the value of the risk averseness level $1-\epsilon$. For these intermediate cases, the horizontal distance with respect to the DMPC strategy depicts the realized thermal comfort improvement, whereas the vertical distance depicts the increase in energy use required to accomplish the enhanced thermal comfort. Figure 4 shows the results of the two different performance assessments proposed in Section 2.4.1: one where the uncertainty on the occupant behavior forecasts is considered (Figure 4a), and one where this uncertainty is ignored (both in the OCP and in the closed-loop simulations) (Figure 4b).

From both Figure 4a and 4b it is immediately clear that there is considerable value in switching from current practice to stochastic approaches (either SMPC^{a} or SMPC^{ap}), because of the clear reduction in thermal comfort violations, indicated by the horizontal span of the trade-off curves. This thermal comfort gain is most pronounced for the cases with a large model uncertainty (indicated by a high WDM index, see Table 3), where the nominal heat demand of the considered building realization is larger than that of the reference model, i.e., especially for samples E and F. Indeed, for these cases, the error induced



(a) With uncertainty on the occupant behavior.



(b) Without uncertainty on the occupant behavior.

Figure 4: Trade-off curves of the thermal comfort violations versus the specific thermal energy demand during the first week of January, for different possible realizations of the studied building.

by disregarding the uncertainties in the DMPC strategy is the largest, because of the combined effect of the incorrect forecasts, the underestimation of the required heat relative to the reference model considered in the OCP, and the incorrect assessment of the moment this heat needs to be delivered (due to an incorrect appraisal of the building dynamics). Nevertheless, also for the other samples, a considerable improvement of thermal comfort is possible.

A large part of this thermal comfort improvement can be attained at the cost of a limited increase of energy use, as indicated by the gentle, almost flat, slope of the trade-off curves; for all building samples, 90% of the thermal comfort improvement relative to the DMPC strategy can be realized with an increase of at most 9% in energy use. However, for larger risk averseness levels ($1 - \epsilon \geq 0.9$), the trade-off between enhanced thermal comfort and additional energy use becomes more pronounced. Overall, for the studied conditions, the increase in energy use of the SMPC^{a} strategy relative to the DMPC strategy for the case with the occupant behavior forecast uncertainty ranges between 0.6% (samples D, E, F, $1 - \epsilon = 0.6$) and 16.7% (sample A, $1-\epsilon = 0.999$, but without complete elimination of thermal discomfort), whereas the relative energy use increase of the SMPC^{ap} approach ranges between 0.7% (samples D, E, F, $1 - \epsilon = 0.6$) and 21.6% (sample A, $1 - \epsilon = 0.999$, with complete elimination of thermal discomfort). For the case without occupant behavior forecast uncertainty, the relative energy use increase of the SMPC^{a} strategy compared to the DMPC strategy ranges between -1.1% (sample A, $1 - \epsilon = 0.6$) and 4.2% (sample A, $1 - \epsilon = 0.999$, but without complete elimination of thermal discomfort), whereas the relative energy use increase of the SMPC^{ap} strategy ranges between -0.3% (samples A, B, $1 - \epsilon = 0.6$) and 13.4% (sample A, $1 - \epsilon = 0.999$, with complete elimination of thermal discomfort); the lower energy use in this case is to be expected, since the omission of part of the uncertainty results in a lower constraint tightening level.

The relative TED increase and TCV decrease of the stochastic approaches compared to the DMPC strategy for all building samples and risk averseness levels are depicted in the subfigures on the right-hand side of Figure 4. Interestingly, all relative trade-off curves of all different building samples more or less coincide; only the curves of samples A and F, being the building samples with the smallest and largest nominal heat demand, show a slightly deviating behavior. Hence, this trend followed by the relative trade-off curves suggests the existence of a rule of thumb when assessing the associated energy cost of an envisioned thermal comfort improvement.

When focussing on the mutual comparison of the two stochastic approaches, a more detailed analysis of Figure 4a shows that for the bulk of the possible building realizations, the added value of the SMPC^{ap} strategy compared to the SMPC^{a} strategy is limited. If thermal comfort improvements by moving from the SMPC^{a} strategy to the SMPC^{ap} strategy of less than 1 K h over an entire week are deemed insufficient, the SMPC^{ap} strategy realizes a considerable thermal comfort improvement only for sample F. When increasing the relative share of the model uncertainty relative to the additive uncertainty, by omitting the uncertainty on the occupant behavior forecast, the improvement brought about by the SMPC^{ap} strategy for sample F is significantly amplified, as shown in Figure 4b. Moreover, also the thermal comfort improvement for sample E becomes substantial. This thermal comfort improvement for samples E and F is attained at a relative energy use increase compared to the SMPC^{a} strategy of 1.7% and 1.6%, respectively, for the case with uncertainty on the occupant behavior; for the other building samples, the relative energy use increase is at most 4.2% in this case. For the case without uncertainty on the occupant behavior, the relative energy use increase for samples E and F amounts to 2.9% and 3.1%, respectively; for the other building samples, the relative increase is at most 8.9%.

To finalize the discussion of the results regarding the optimal control performance, it is important to stress that the results above are heavily affected by two implicit assumptions, which hamper the SMPC^{ap} strategy to fully distinguish itself from the SMPC^{a} strategy, being i) that the stochastic OCP is re-solved for every subsequent time step, and ii) that the heat supply system has sufficient heating capacity available. The less frequently the OCP is being solved (e.g., when implementing the calculated ADF strategy over a certain horizon rather than re-optimizing the control strategy every time step), and/or the more limited the available heating capacity is, the more important a correct uncertainty anticipation becomes to guarantee a good control performance.

3.2 Optimal design performance assessment

Figure 5 visualizes the thermal discomfort ranges to be used to make a design decision, resulting from the application of the PBMPC, DMPC, SMPC^{a} or SMPC^{ap} strategy during the 18th of January for different capacities of the heat supply system. Multiple observations can be made indicating the added value of using the SMPC^{ap} strategy for optimal design applications.

From Figure 5, it becomes clear that depending on the applied MPC strategy, a different heat supply system size will be chosen. According to the PBMPC strategy, a heat supply system with a thermal power of 13 kW is able to guarantee thermal comfort for all building samples. However, this is a false promise; when taking into account the closed-loop impact of the uncertainties, by rather looking at the results of the DMPC strategy, it is clear that this system size in reality leads to considerable thermal discomfort. For the DMPC strategy, this thermal discomfort can be decreased, but evidently never eliminated[18], by switching to a larger system size, where the design guaranteeing the lowest TCV is the largest considered size of 15 kW. When looking at the SMPC^{a} and SMPC^{ap} strategies, where the closed-loop impact of (part of) the uncertainties is not only taken into account, but also explicitly anticipated for, Figure 5 shows that these MPC strategies can further reduce the thermal discomfort, where the SMPC^{ap} strategy is even able to truly guarantee zero thermal discomfort for all building samples for a risk averseness level $1-\epsilon = 0.999$ and an installed power of 14 kW, in contrast to the PBMPC, DMPC or SMPC^{a} strategy. Taking the thermal discomfort of the DMPC strategy with a system size of 15 kW as a reference, indicated by the grey dashed horizontal line in Figure 5, the same degree of thermal discomfort only occurs at a system size of 12 kW down to 11 kW for the SMPC^{a} strategy, and of 11 kW down to 10 kW for the SMPC^{ap} strategy, depending on the applied risk averseness level[19].

The reason why the stochastic approaches are able to longer avoid thermal discomfort, is because of their fundamentally different way of working compared to a deterministic approach, as illustrated by Figure 6. The DMPC strategy does not anticipate for any uncertainty in its open-loop OCP, and hence waits until the last possible moment to start heating, to subsequently fully exploit the maximum available power. In case the required real-time correction/additional heating thereupon exceeds the capacity of the heating system, thermal discomfort occurs. This effect (evidently) becomes more pronounced for smaller heat supply system sizes[20]. In contrast, stochastic MPC approaches explicitly optimize both the anticipation for as well as the reaction against uncertainties (via ADF) in their open-loop OCP. As such, they deploy the available thermal power in a better way. The pronounced anticipative behavior of the stochastic approaches, and of the SMPC^{ap} strategy in particular, can be clearly distinguished in Figure 6, especially for smaller heating capacities[21]. These observations confirm the assertion made at the end of the discussion of the first case study, stating that the added value of the SMPC^{ap} strategy compared to the SMPC^{a} strategy depends on the required degree of anticipation, which is, among others, influenced by the available heating capacity. Indeed, Figure 7 clearly shows that, because the SMPC^{ap} strategy is able to longer avoid thermal discomfort compared to the SMPC^{a} strategy, the difference in TCV between the two approaches becomes more pronounced for decreasing heating capacities, up to the point where also the SMPC^{ap} strategy is no longer able to guarantee thermal comfort. Figure 7 also shows that this improved performance of the SMPC^{ap} strategy comes at the cost of a higher TED, due to the increased losses associated with the more pronounced anticipative behavior.

The final decision about the most appropriate design is a complex issue, depending on different (and possibly conflicting) factors, including: i) the user's and designer's preference regarding the amount of ther-

[18] Deterministic approaches do not hedge against uncertainty, making thermal discomfort due to closed-loop perturbations inevitable.

[19] Similar thermal discomfort levels can be obtained for different combinations of system sizes and risk averseness levels (where the risk averseness level is rather a control preference characteristic to the user), illustrating the interchangeability between control and design.

[20] This explains the need for larger system sizes in case of a DMPC strategy: to be able to correct for wrong control strategies, real-time flexibility is required in the form of spare capacity.

[21] Also the DMPC strategy shows a certain degree of anticipation. However, this anticipation has nothing to do with uncertainties, but is merely due to the fact that the decreasing installed power becomes insufficient to deliver an instanteneous heat power peak.

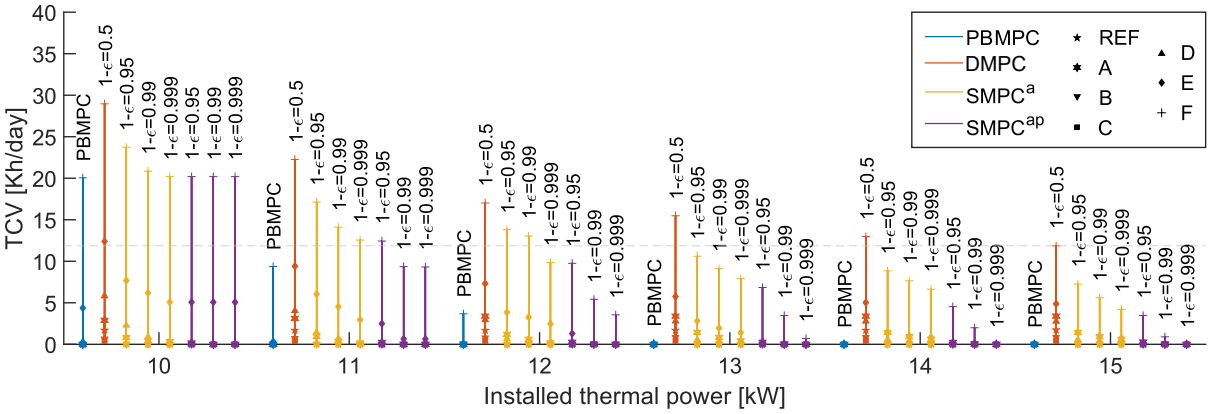


Figure 5: Thermal discomfort ranges showing the TCV for different possible realizations of the studied building, as a function of the installed thermal power of the heat supply system, applied MPC strategy (PBMPC, DMPC, SMPC^{a} or SMPC^{ap}) and imposed risk averseness level.

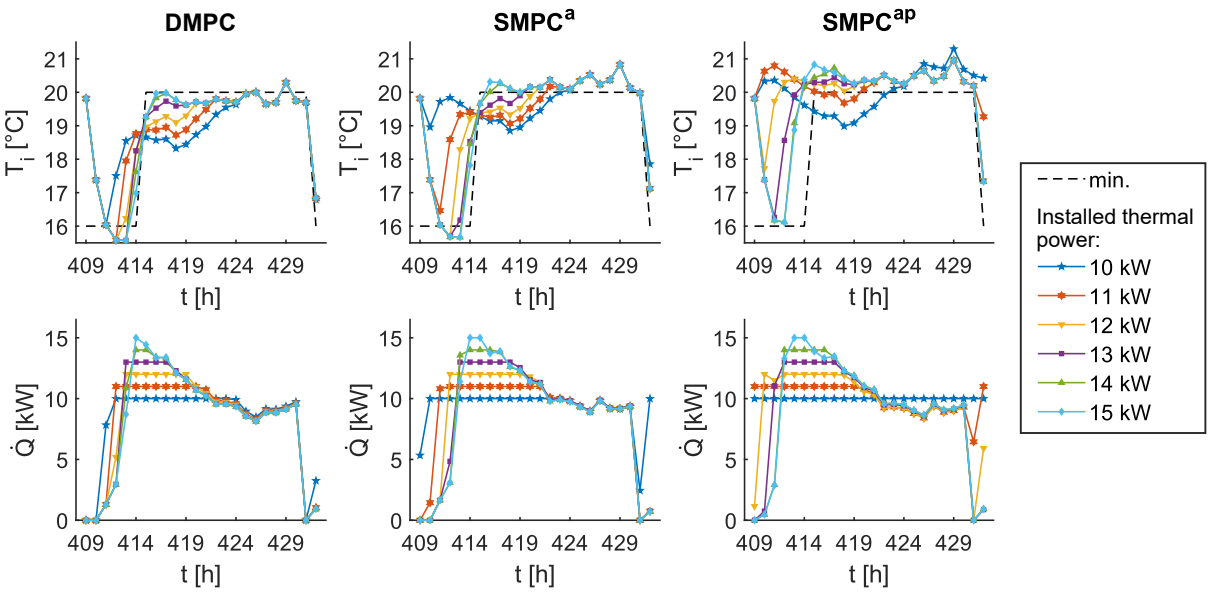


Figure 6: The closed-loop indoor temperature profile and heat input profile realized during the 18th of January for different installed powers of the heat supply system.

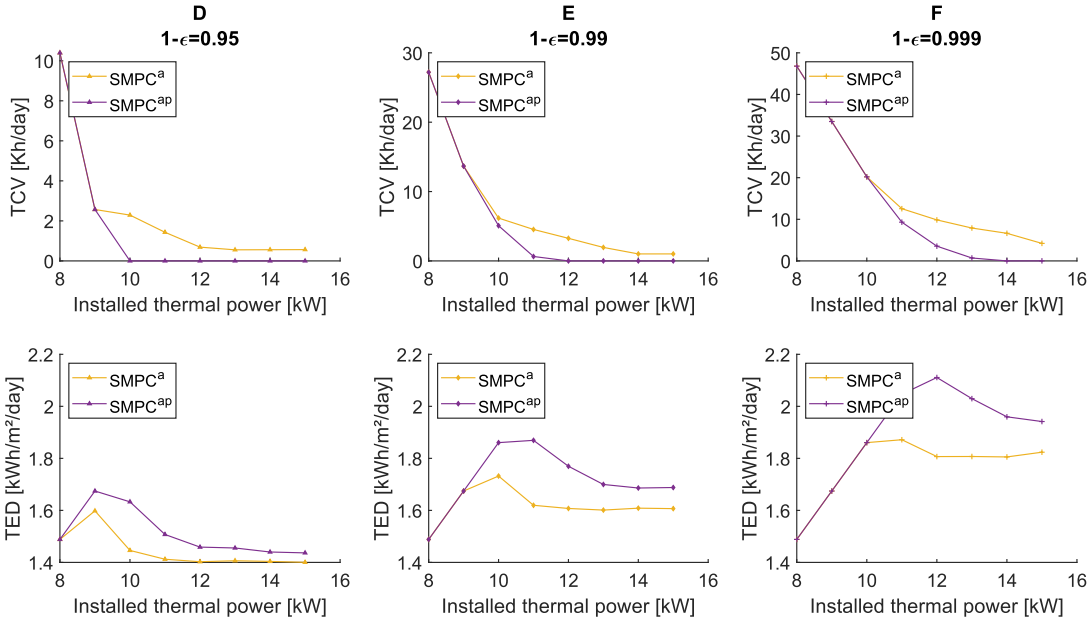


Figure 7: The differentiation between the control performance of the SMPC^{a} strategy and SMPC^{ap} strategy in terms of TCV and TED as a function of the installed thermal power for samples D, E and F of the studied building.

mal discomfort that is allowed (i.e., is it preferred to guarantee thermal comfort for all possible building realizations, or are certain building realizations - e.g., the most uncertain/extreme ones - rather disregarded when making a design decision?), ii) the investment cost, determined by the heat supply system size, and iii) the operational cost, determined by the control choices (i.e., which MPC strategy, and which risk averseness level). Especially the latter two aspects require a careful balancing, since a smaller heating capacity results in a smaller investment cost, but requires a control approach enforcing increased anticipative behavior, resulting in a higher operational cost if a constant tariff structure is in place[22]. In analogy with the vision adopted for chance constrained optimal control, this whole sizing problem could be tackled via a chance constrained optimal design problem, by properly implementing an IOCD approach, where the investment costs and operational costs are weighed up. Based on the auspicious results obtained in this exploratory case study, this is considered as a valuable future research track, which is out of scope of this study.

[22] With a variable energy price, a higher energy use could result in a lower energy cost.

4 Conclusion

Although the building model parameters are recognized as an important source of uncertainty affecting building energy performance, in addition to the uncertainty associated with the forecasts of the disturbances (i.e., weather and occupant behavior), this parametric uncertainty is only occasionally explicitly addressed in model predictive control applications for building climate control. Therefore, this paper develops and assesses a more dedicated stochastic model predictive control approach for building climate control under combined parametric and additive uncertainty, SMPC^{ap}, tailored to the class of systems represented by a linear time-invariant state space model. To this end, the nominal, deterministic optimal control problem formulation is converted into its stochastic equivalent, explicitly accounting for all relevant uncertainties. In addition, a mathematical uncertainty characterization of the building model parameters, the weather forecasts and the occupant behavior forecasts is derived. To fully appraise the potential added value of the SMPC^{ap} strategy, its performance is assessed in two case studies. From an optimal control perspective, the enhanced uncertainty antic-

ipation of the SMPC^{ap} strategy is shown to induce improved thermal comfort compared to the current practice deterministic MPC strategy and the state-of-the-art SMPC^{a} strategy only accounting for additive uncertainties, and this at the expense of a limited increase in energy use. For the considered cases, 90% of the thermal comfort improvement compared to the deterministic MPC strategy can be attained with a relative increase of at most 9% in energy use; the maximum relative increase in energy use amounts to 21.6% relative to the deterministic MPC strategy, and 4.2% relative to the SMPC^{a} strategy. The added value of the SMPC^{ap} strategy is shown to be most pronounced for buildings with a large model uncertainty and nominal heat demand, and/or for buildings equipped with a heat supply system with a limited heating capacity. Second, from an optimal design perspective, the suitability of the SMPC^{ap} strategy for obtaining a more appropriate, yet robust, heat supply system size is illustrated. By incorporating the SMPC^{ap} strategy in an integrated optimal control and design approach, size reductions of 4 up to 5 kW (or in relative terms, up to 33.3%) are possible for a heating system initially sized at 15 kW, installed in a terraced single-family dwelling, without increasing thermal discomfort compared to an equivalent approach incorporating a deterministic MPC strategy. Based on the results of this exploratory case study, illustrating the capability of the SMPC^{ap} strategy to longer hold off thermal comfort deteriorations compared to other control strategies, chance constrained integrated optimal control and design is advocated as a valuable future research track.

5 Future work

This work demonstrates the upper limits of the feasible thermal comfort improvement and associated energy costs, and of the feasible equipment sizing saving, brought about by the developed SMPC^{ap} strategy, via simulations. An important next step is bringing the proposed methodology into practice. Here, the use of data-driven approaches/machine learning may be a key enabler, in order to derive the stochastic building model and/or the additive uncertainty representation to be used by the SMPC^{ap} strategy. In this setting, the uncertainty characterizations derived in this paper can serve as substantiated initial guesses, which can be subsequently updated in an online fashion.

Acknowledgements

This work was supported by KU Leuven (C2 Research Project C24/16/018 'Energy Storage as a Disruptive Technology in the Energy System of the Future') and the Research Foundation – Flanders (FWO) (postdoctoral mandate 12J3320N). Besides, the resources and services used in this work were provided by the VSC (Flemish Supercomputer Center), funded by the Research Foundation - Flanders (FWO) and the Flemish Government.

Disclosure statement

No potential conflict of interest was reported by the authors.

ORCID

Anke Uytterhoeven

Robbe Van Rompaey

Kenneth Bruninx

Lieve Helsen

References

[1] A. Afram and F. Janabi-Sharifi, "Theory and applications of HVAC control systems – A review of model predictive control (MPC)," *Building and Environment*, vol. 72, pp. 343–355, 2014.

[2] G. Serale, M. Fiorentini, A. Capozzoli, D. Bernardini, and A. Bemporad, "Model predictive control (MPC) for enhancing building and HVAC system energy efficiency: Problem formulation, applications and opportunities," *Energies*, vol. 11, no. 3, p. 631, 2018.

[3] J. Drgoňa, J. Arroyo, I. C. Figueroa, D. Blum, K. Arendt, D. Kim, E. P. Ollé, J. Oravec, M. Wetter, D. L. Vrabie, *et al.*, "All you need to know about model predictive control for buildings," *Annual Reviews in Control*, 2020.

[4] H. Thieblemont, F. Haghighat, R. Ooka, and A. Moreau, "Predictive control strategies based on weather forecast in buildings with energy storage system: A review of the state-of-the art," *Energy and Buildings*, vol. 153, pp. 485–500, 2017.

[5] A. Mirakhorli and B. Dong, "Occupancy behavior based model predictive control for building indoor climate—a critical review," *Energy and Buildings*, vol. 129, pp. 499–513, 2016.

[6] C. D. Korkas, S. Baldi, I. Michailidis, and E. B. Kosmatopoulos, "Occupancy-based demand response and thermal comfort optimization in microgrids with renewable energy sources

and energy storage," *Applied Energy*, vol. 163, pp. 93–104, 2016.

[7] F. Oldewurtel, A. Ulbig, A. Parisio, G. Andersson, and M. Morari, "Reducing peak electricity demand in building climate control using real-time pricing and model predictive control," in *49th IEEE conference on decision and control (CDC), Atlanta, GA, USA*, pp. 1927–1932, IEEE, 2010.

[8] G. Bianchini, M. Casini, A. Vicino, and D. Zarrilli, "Demand-response in building heating systems: A Model Predictive Control approach," *Applied Energy*, vol. 168, pp. 159–170, 2016.

[9] M. Avci, M. Erkoc, A. Rahmani, and S. Asfour, "Model predictive HVAC load control in buildings using real-time electricity pricing," *Energy and Buildings*, vol. 60, pp. 199–209, 2013.

[10] S. Bengea, V. Adetola, K. Kang, M. J. Liba, D. Vrabie, R. Bitmead, and S. Narayanan, "Parameter estimation of a building system model and impact of estimation error on closed-loop performance," in *50th IEEE Conference on Decision and Control and European Control Conference, 2011, Orlando, FL, USA*, pp. 5137–5143, IEEE, 2011.

[11] F. Oldewurtel, D. Gyalistras, M. Gwerder, C. Jones, A. Parisio, V. Stauch, B. Lehmann, and M. Morari, "Increasing energy efficiency in building climate control using weather forecasts and model predictive control," in *Clima-RHEVA World Congress, 2010, Antalya, Turkey*, 2010.

[12] F. Oldewurtel, A. Parisio, C. N. Jones, D. Gyalistras, M. Gwerder, V. Stauch, B. Lehmann, and M. Morari, "Use of model predictive control and weather forecasts for energy efficient building climate control," *Energy and Buildings*, vol. 45, pp. 15–27, 2012.

[13] S. Goyal, H. A. Ingley, and P. Barooah, "Effect of various uncertainties on the performance of occupancy-based optimal control of HVAC zones," in *2012 IEEE 51st IEEE conference on decision and control (CDC)*, pp. 7565–7570, IEEE, 2012.

[14] M. Prandini, S. Garatti, and J. Lygeros, "A randomized approach to stochastic model predictive control," in *2012 IEEE 51st IEEE Conference on Decision and Control (CDC)*, pp. 7315–7320, IEEE, 2012.

[15] X. Zhang, S. Grammatico, G. Schildbach, P. Goulart, and J. Lygeros, "On the sample size of randomized MPC for chance-constrained systems with application to building climate control," in *2014 European Control Conference (ECC)*, pp. 478–483, 2014.

[16] D. Ioli, A. Falsone, and M. Prandini, "Energy management of a building cooling system with thermal storage: a randomized solution with feedforward disturbance compensation," in *2016 American Control Conference (ACC)*, pp. 2346–2351, IEEE, 2016.

[17] J. Zhang and T. Ohtsuka, "Stochastic model predictive control using simplified affine disturbance feedback for chance-constrained systems," *IEEE Control Systems Letters*, vol. 5, no. 5, pp. 1633–1638, 2020.

[18] L. Hewing, K. P. Wabersich, and M. N. Zeilinger, "Recursively feasible stochastic model predictive control using indirect feedback," *Automatica*, vol. 119, p. 109095, 2020.

[19] M. Maasoumy and A. Sangiovanni-Vincentelli, "Optimal control of building HVAC systems in the presence of imperfect predictions," in *Dynamic Systems and Control Conference*, vol. 45301, pp. 257–266, American Society of Mechanical Engineers, 2012.

[20] X. Zhang, G. Schildbach, D. Sturzenegger, and M. Morari, "Scenario-based MPC for energy-efficient building climate control under weather and occupancy uncertainty," in *2013 European Control Conference (ECC)*, pp. 1029–1034, 2013.

[21] Y. Long, S. Liu, L. Xie, and K. H. Johansson, "A scenario-based distributed stochastic MPC for building temperature regulation," in *2014 IEEE international conference on automation science and engineering (CASE)*, pp. 1091–1096, IEEE, 2014.

[22] A. Parisio, M. Molinari, D. Varagnolo, and K. H. Johansson, "A scenario-based predictive control approach to building HVAC management systems," in *2013 IEEE International Conference on Automation Science and Engineering (CASE)*, pp. 428–435, IEEE, 2013.

[23] Y. Ma, J. Matuško, and F. Borrelli, "Stochastic model predictive control for building HVAC systems: Complexity and conservatism," *IEEE Transactions on Control Systems Technology*, vol. 23, no. 1, pp. 101–116, 2014.

[24] F. Oldewurtel, C. N. Jones, A. Parisio, and M. Morari, "Stochastic model predictive control for building climate control," *IEEE Transactions on Control Systems Technology*, vol. 22, no. 3, pp. 1198–1205, 2013.

[25] A. Ioannou and L. C. Itard, "Energy performance and comfort in residential buildings: Sensitivity for building parameters and occupancy," *Energy and Buildings*, vol. 92, pp. 216–233, 2015.

[26] W. Tian, Y. Heo, P. De Wilde, Z. Li, D. Yan, C. S. Park, X. Feng, and G. Augenbroe, "A review of uncertainty analysis in building energy assessment," *Renewable and Sustainable Energy Reviews*, vol. 93, pp. 285–301, 2018.

[27] M. Maasoumy, M. Razmara, M. Shahbakhti, and A. S. Vincentelli, "Handling model uncertainty in model predictive control for energy efficient buildings," *Energy and Buildings*, vol. 77, pp. 377–392, 2014.

[28] M. Tanaskovic, D. Sturzenegger, R. Smith, and M. Morari, "Robust adaptive model predictive building climate control," *IFAC-PapersOnLine*, vol. 50, no. 1, pp. 1871–1876, 2017.

[29] H. Nagpal, A. Staino, and B. Basu, "Robust model predictive control of HVAC systems with uncertainty in building parameters using linear matrix inequalities," *Advances in Building Energy Research*, vol. 14, no. 3, pp. 338–354, 2020.

[30] S. Yang, M. P. Wan, W. Chen, B. F. Ng, and D. Zhai, "An adaptive robust model predictive control for indoor climate optimization and uncertainties handling in buildings," *Building and Environment*, vol. 163, p. 106326, 2019.

[31] I. De Jaeger, *On the Impact of Input Data Uncertainty on the Reliability of Urban Building Energy Models*. PhD thesis, KU Leuven, 2021.

[32] M. Killian and M. Kozek, "Ten questions concerning model predictive control for energy efficient buildings," *Building and Environment*, vol. 105, pp. 403–412, 2016.

[33] F. Jorissen, W. Boydens, and L. Helsen, "Methodology for integrated optimal control and design of buildings," in *Proceedings of the REHVA Annual Meeting Conference Low Carbon Technologies in HVAC, ATIC, Brussels*, 2018.

[34] B. van der Heijde, *Optimal Integration of Thermal Energy Storage and Conversion in Fourth Generation Thermal Networks.* PhD thesis, KU Leuven, 2019.

[35] NBN, "NBN EN ISO 15251:2007 - Indoor environmental input parameters for design and assessment of energy performance of buildings addressing indoor air quality, thermal environment, lighting and acoustics," 2007.

[36] P. Huang, G. Huang, and Y. Wang, "HVAC system design under peak load prediction uncertainty using multiple-criterion decision making technique," *Energy and Buildings*, vol. 91, pp. 26–36, 2015.

[37] Y. Sun, L. Gu, C. J. Wu, and G. Augenbroe, "Exploring HVAC system sizing under uncertainty," *Energy and Buildings*, vol. 81, pp. 243–252, 2014.

[38] E. Djunaedy, K. Van den Wymelenberg, B. Acker, and H. Thimmana, "Oversizing of HVAC system: signatures and penalties," *Energy and Buildings*, vol. 43, no. 2-3, pp. 468–475, 2011.

[39] W. Gang, S. Wang, K. Shan, and D. Gao, "Impacts of cooling load calculation uncertainties on the design optimization of building cooling systems," *Energy and Buildings*, vol. 94, pp. 1–9, 2015.

[40] W. Gang, S. Wang, F. Xiao, and D.-c. Gao, "Robust optimal design of building cooling systems considering cooling load uncertainty and equipment reliability," *Applied Energy*, vol. 159, pp. 265–275, 2015.

[41] NBN, "NBN EN ISO 7730:2005 - Ergonomics of the thermal environment - Analytical determination and interpretation of thermal comfort using calculation of the PMV and PPD indices and local thermal comfort criteria," 2005.

[42] I. De Jaeger, J. Lago, and D. Saelens, "A probabilistic approach to allocate building parameters within district energy simulations," in *Proceedings of the Urban Energy Simulation Conference, 2018, Glasgow, Scotland*, University of Strathclyde, 2018.

[43] I. De Jaeger, J. Lago, and D. Saelens, "A probabilistic building characterization method for district energy simulations," *Energy and Buildings*, vol. 230, p. 110566, 2021.

[44] G. Mavromatidis, K. Orehounig, and J. Carmeliet, "A review of uncertainty characterisation approaches for the optimal design of distributed energy systems," *Renewable and Sustainable Energy Reviews*, vol. 88, pp. 258–277, 2018.

[45] S. Petersen and K. W. Bundgaard, "The effect of weather forecast uncertainty on a predictive control concept for building systems operation," *Applied Energy*, vol. 116, pp. 311–321, 2014.

[46] F. Oldewurtel, *Stochastic model predictive control for energy efficient building climate control.* PhD thesis, ETH Zurich, Zürich, 2011. Diss., Eidgenössische Technische Hochschule ETH Zürich, Nr. 19908, 2011.

[47] A. Mesbah, "Stochastic model predictive control: An overview and perspectives for future research," *IEEE Control Systems Magazine*, vol. 36, no. 6, pp. 30–44, 2016.

[48] C. E. Rasmussen and C. K. I. Williams, *Gaussian Processes for Machine Learning*. Massachusetts Institute of Technology, 2006. Appendix A: Mathematical background.

[49] R. A. Horn and C. R. Johnson, "Topics in matrix analysis," *Cambridge University Presss, Cambridge*, vol. 37, p. 39, 1991.

[50] M. Farina, L. Giulioni, and R. Scattolini, "Stochastic linear model predictive control with chance constraints–a review," *Journal of Process Control*, vol. 44, pp. 53–67, 2016.

[51] W. K. Klein Haneveld, M. H. van der Vlerk, and W. Romeijnders, *Chance Constraints*, pp. 115–138. Cham: Springer International Publishing, 2020.

[52] F. Oldewurtel, C. N. Jones, and M. Morari, "A tractable approximation of chance constrained stochastic MPC based on affine disturbance feedback," in *2008 47th IEEE conference on decision and control*, pp. 4731–4736, IEEE, 2008.

[53] Y. Ma, S. Vichik, and F. Borrelli, "Fast stochastic MPC with optimal risk allocation applied to building control systems," in *2012 IEEE 51st IEEE Conference on Decision and Control (CDC)*, pp. 7559–7564, IEEE, 2012.

[54] X. Geng and L. Xie, "Data-driven decision making in power systems with probabilistic guarantees: Theory and applications of chance-constrained optimization," *Annual Reviews in Control*, vol. 47, pp. 341–363, 2019.

[55] A. Parisio, D. Varagnolo, D. Risberg, G. Pattarello, M. Molinari, and K. H. Johansson, "Randomized model predictive control for HVAC systems," in *Proceedings of the 5th ACM Workshop on Embedded Systems For Energy-Efficient Buildings*, pp. 1–8, 2013.

[56] A. Parisio, D. Varagnolo, M. Molinari, G. Pattarello, L. Fabietti, and K. H. Johansson, "Implementation of a scenario-based MPC for HVAC systems: an experimental case study," *IFAC Proceedings Volumes*, vol. 47, no. 3, pp. 599–605, 2014.

[57] J. Drgoňa, M. Kvasnica, M. Klaučo, and M. Fikar, "Explicit stochastic MPC approach to building temperature control," in *52nd IEEE Conference on Decision and Control*, pp. 6440–6445, 2013.

[58] M. Farina and R. Scattolini, "Model predictive control of linear systems with multiplicative unbounded uncertainty and chance constraints," *Automatica*, vol. 70, pp. 258–265, 2016.

[59] A. Nemirovski and A. Shapiro, "Convex approximations of chance constrained programs," *SIAM Journal on Optimization*, vol. 17, no. 4, pp. 969–996, 2007.

[60] G. C. Calafiore and L. El Ghaoui, "On distributionally robust chance-constrained linear programs," *Journal of Optimization Theory and Applications*, vol. 130, no. 1, pp. 1–22, 2006.

[61] S. Peng, *Chance constrained problem and its applications*. PhD thesis, Université Paris Saclay (COmUE); Xi'an Jiaotong University, 2019.

[62] F. Oldewurtel, A. Parisio, C. N. Jones, M. Morari, D. Gyalistras, M. Gwerder, V. Stauch, B. Lehmann, and K. Wirth, "Energy efficient building climate control using stochastic model predictive control and weather predictions," in *Proceedings of the 2010 American control conference*, pp. 5100–5105, IEEE, 2010.

[63] G. Reynders, J. Diriken, and D. Saelens, "Quality of grey-box models and identified parameters as function of the accuracy of input and observation signals," *Energy and Buildings*, vol. 82, pp. 263–274, 2014.

[64] P. Bacher and H. Madsen, "Identifying suitable models for the heat dynamics of buildings," *Energy and Buildings*, vol. 43, no. 7, pp. 1511–1522, 2011.

[65] H. Harb, N. Boyanov, L. Hernandez, R. Streblow, and D. Müller, "Development and validation of grey-box models for forecasting the thermal response of occupied buildings," *Energy and Buildings*, vol. 117, pp. 199–207, 2016.

[66] A. Tindale, "Third-order lumped-parameter simulation method," *Building Services Engineering Research and Technology*, vol. 14, no. 3, pp. 87–97, 1993.

[67] G. Reynders, *Quantifying the impact of building design on the potential of structural storage for active demand response in residential buildings*. PhD thesis, KU Leuven, 2015.

[68] M. Gouda, S. Danaher, and C. Underwood, "Low-order model for the simulation of a building and its heating system," *Building Services Engineering Research and Technology*, vol. 21, no. 3, pp. 199–208, 2000.

[69] G. Reynders, J. Diriken, and D. Saelens, "Bottom-up modeling of the belgian residential building stock: influence of model complexity," in *Proceedings of the 9th International Conference on System Simulation in Buildings, 2014, Liège, Belgium*, pp. 1–19, University of Liège, 2014.

[70] O. Gutschker, "Parameter identification with the software package LORD," *Building and Environment*, vol. 43, no. 2, pp. 163 – 169, 2008. Outdoor Testing, Analysis and Modelling of Building Components.

[71] M. J. Jiménez, H. Madsen, and K. K. Andersen, "Identification of the main thermal characteristics of building components using matlab," *Building and Environment*, vol. 43, no. 2, pp. 170–180, 2008.

[72] A. Uytterhoeven, I. De Jaeger, K. Bruninx, D. Saelens, and L. Helsen, "Data-driven estimation of parametric uncertainty of reduced order RC models for building climate control (in press)," in *Proceedings of the International Building Performance Simulation Association*, International Building Performance Association (IBPSA), 2021.

[73] W. Lambrichts, "Model Predictive Control of Residential Heating: Accounting for Uncertainties on Weather and Occupancy Behaviour," Master's thesis, KU Leuven, 2020.

[74] O. Guerra-Santin and L. Itard, "Occupants' behaviour: determinants and effects on residential heating consumption," *Building Research & Information*, vol. 38, no. 3, pp. 318–338, 2010.

[75] A. E.-D. Mady, G. Provan, C. Ryan, and K. Brown, "Stochastic model predictive controller for the integration of building use and temperature regulation," in *Proceedings of the AAAI Conference on Artificial Intelligence*, vol. 25, 2011.

[76] R. Baetens and D. Saelens, "Modelling uncertainty in district energy simulations by stochastic residential occupant behaviour," *Journal of Building Performance Simulation*, vol. 9, no. 4, pp. 431–447, 2016.

[77] L. Peeters, R. De Dear, J. Hensen, and W. D'haeseleer, "Thermal comfort in residential buildings: Comfort values and scales for building energy simulation," *Applied energy*, vol. 86, no. 5, pp. 772–780, 2009.

[78] NBN, "NBN EN 12831-1: Energy performance of buildings - Method for calculation of the design heat load - Part 1: Space heating load," 2017.